Biochemical and Biophysical Research Communications 390 (2009) 636–641

Contents lists available at ScienceDirect

Biochemical and Biophysical Research Communications

journal homepage: www.elsevier.com/locate/ybbrc

An animal model of preclinical diagnosis of pancreatic ductal adenocarcinomas

Katsumi Fukamachi [a], Hajime Tanaka [b], Yoshiaki Hagiwara [d,e], Hirotaka Ohara [b], Takashi Joh [b], Masaaki Iigo [a], David B. Alexander [a], Jiegou Xu [a], Ne Long [a], Misato Takigahira [f,g], Kazuyoshi Yanagihara [f,h], Okio Hino [e], Izumu Saito [i], Hiroyuki Tsuda [a,c,*]

[a] Department of Molecular Toxicology, Nagoya City University Graduate School of Medical Sciences, 1 Kawasumi, Mizuho-cho, Mizuho-ku, Nagoya 467-8601, Japan
[b] Department of Gastroenterology and Metabolism, Nagoya City University Graduate School of Medical Sciences, 1 Kawasumi, Mizuho-cho, Mizuho-ku, Nagoya 467-8601, Japan
[c] Nanotoxicology Project, Nagoya City University Graduate School of Medical Sciences, 1 Kawasumi, Mizuho-cho, Mizuho-ku, Nagoya 467-8601, Japan
[d] Immuno-Biological Laboratories, 5-1 Aramachi, Takasaki-Shi, Gunma 370-0831, Japan
[e] Department of Pathology and Oncology, Juntendo University School of Medicine, 2-1-1 Hongo, Tokyo 113-8421, Japan
[f] Central Animal Laboratory, National Cancer Center Research Institute, 5-1-1 Tsukiji, Chuo-ku, Tokyo 104-0045, Japan
[g] Gastrointestinal Section, National Cancer Center Hospital, 5-1-1 Tsukiji, Chuo-ku, Tokyo 104-0045, Japan
[h] Laboratory of Health Sciences, Department of Life Sciences, Yasuda Women's University, 6-13-1 Yasuhigashi, Asaminami-ku, Hiroshima 731-0153, Japan
[i] Laboratory of Molecular Genetics, Institute of Medical Science, University of Tokyo, 4-6-1 Shirokanedai, Minato-ku, Tokyo 108-8639, Japan

ARTICLE INFO

Article history:
Received 3 October 2009
Available online 8 October 2009

Keywords:
Pancreas cancer
Serum marker
Erc
Mesothelin
Animal model

ABSTRACT

Pancreatic ductal adenocarcinoma (PDA) is a highly lethal disease, which is usually diagnosed in an advanced stage. Animal PDA models which reflect the human condition are clearly necessary to develop early diagnostic tools and explore new therapeutic approaches. We have established transgenic rats carrying a mutated H- or K-*ras* gene (Hras250 and Kras327) controlled by Cre/loxP activation. These animals develop PDA which are histopathologically similar to that in humans. We utilized this model to identify biomarkers to detect early PDA. We report here that serum levels of Erc/Mesothelin are significantly higher in rats bearing PDA than in controls. Importantly, the levels are significantly elevated in rats before grossly visible carcinomas develop. Even in rats with very small microscopic ductal carcinoma lesions, elevated serum Erc/Mesothelin can be detected. We believe this is the first report of a pancreas tumor animal model in which pre-symptomatic lesions can be diagnosed.

Introduction

Pancreatic ductal adenocarcinoma (PDA) carries the most dismal prognosis of all solid tumors. Preclinical detection of PDA is a necessary first step toward more successful treatment of this disease. Late manifestation of clinical symptoms, as well as the rapid and aggressive course of the disease contribute to its extremely high mortality. Most patients die within 1 year of diagnosis [1], and the 5 year survival rate is <5% [2]. Since the pancreas is located in a retroperitoneal cavity, detection of the tumor mass is possible only when it has reached a relatively large size. Furthermore, markers for the diagnosis of PDA have not yet been established. Consequently, diagnosis of pancreatic cancers when they are still treatable is extremely rare [3].

We have established transgenic rat lines carrying a human $Hras^{G12V}$ (Hras250) [4] or a human $Kras^{G12V}$ (Kras327) oncogene in which the expression of the transgene is regulated by the Cre/loxP system (termed *ras* Tg rats). Targeted activation of the transgene is accomplished by injection of a Cre recombinase-carrying adenovirus (AxCANCre) into the pancreatic ducts through the common bile duct. Neoplastic lesions in the *ras* Tg rats exhibit morphological similarities to those observed in human pancreas lesions. Early ductal lesions exhibit close similarity to intraepithelial neoplasias (PanIN category).

The rat *Erc* (expressed in renal cell carcinoma) gene was identified as a highly expressed gene in renal cell carcinoma of the Eker rat [5,6]. A human homolog of rat *Erc* is the *Mesothelin/megakaryocyte potentiating factor* (*MPF*) gene [7,8]. Mesothelin was identified as a cell surface antigen recognized by the monoclonal antibody K1 in human mesotheliomas and ovarian carcinomas [9–11]; MPF was independently identified in the culture supernatant of a human pancreatic carcinoma cell line, HPC-Y5 [12]. Human Mesothelin/MPF is derived from a common 71 kDa precursor [8,11]. The precursor protein is cleaved by a furin-like protease, and a 31 kDa NH_2-terminal peptide (MPF) is released into the extracellular

Abbreviations: PanIN, pancreatic intraepithelial neoplasias; PDA, pancreas ductal adenocarcinoma; AxCANCre, Cre recombinase-carrying adenovirus; TEF-1, transcription enhancer factor-1

* Corresponding author. Address: Nanotoxicology Project, Nagoya City University Graduate School of Medical Sciences, 1 Kawasumi, Mizuho-cho, Mizuho-ku, Nagoya 467-8601, Japan. Fax: +81 52 853 8996.
E-mail address: htsuda@med.nagoya-cu.ac.jp (H. Tsuda).

0006-291X/$ - see front matter © 2009 Elsevier Inc. All rights reserved.
doi:10.1016/j.bbrc.2009.10.019

space, leaving a 40 kDa COOH-terminal peptide (Mesothelin) attached to the cell surface by a GPI-anchor [9]. To avoid confusion, we refer to the rat Erc protein and its human homolog as Erc/Mesothelin. Erc/Mesothelin is expressed in ovary and pancreas carcinoma tissue in humans [13–15] and can be used as a marker for PDA [15]. Recently, we developed a novel sandwich ELISA system for serum Erc/Mesothelin [16–19]. Using this serum assay system, the level of Erc/Mesothelin was found to be higher in samples from mesothelioma patients than in samples from subjects without pancreas lesions [16,17]. In the present study we report the use of Erc/Mesothelin as a reliable serum marker for pre-symptomatic, pre-malignant pancreas lesions in *ras* Tg rats.

Materials and methods

Animals. Male Hras^{G12V} transgenic (Hras250) rats were bred with female Sprague–Dawley rats by CLEA Japan Inc. (Tokyo, Japan) as previously reported [4]. Routine genotyping of Hras250 rats was performed using the primers 5′-TCGTGCTTTACGGTATCGCCGCTCCC GATT-3′ and 5′-GATCTGCTCCCTGTACTGGTGG-3′. For the generation of transgenic rats conditionally expressing human Kras^{G12V}, 3× hemagglutinin (HA) tagged Kras^{G12V} cDNA was subcloned into the SacI/KpnI site of pCALNL5 (DNA Bank, RIKEN BioResource Center, Ibaraki, Japan). The purified cassette was injected into the pronuclei of Sprague–Dawley rats (CLEA Japan, Tokyo, Japan) as previously reported [4,20]. Two lines were established (Kras301 and Kras327). In this study, we used the Kras327 line. Routine genotyping of Kras327 rats was performed using the primers 5′-TCTGGATCAAATCCGAAC GC-3′ and 5′-TGACCTGCTGTGTCGAGAAT-3′. Rats were maintained in plastic cages in an air-conditioned room with a 12-h light/12-h dark cycle. The experiments were conducted according to the 'Guidelines for Animal Experiments of the Nagoya City University Graduate School of Medical Sciences'.

Tumor induction and pathological examination. AxCANCre was amplified in HEK293 cells and then purified using Vivapure Adenopack (Vivascience, Hannover, Germany). The titer of the adenovirus

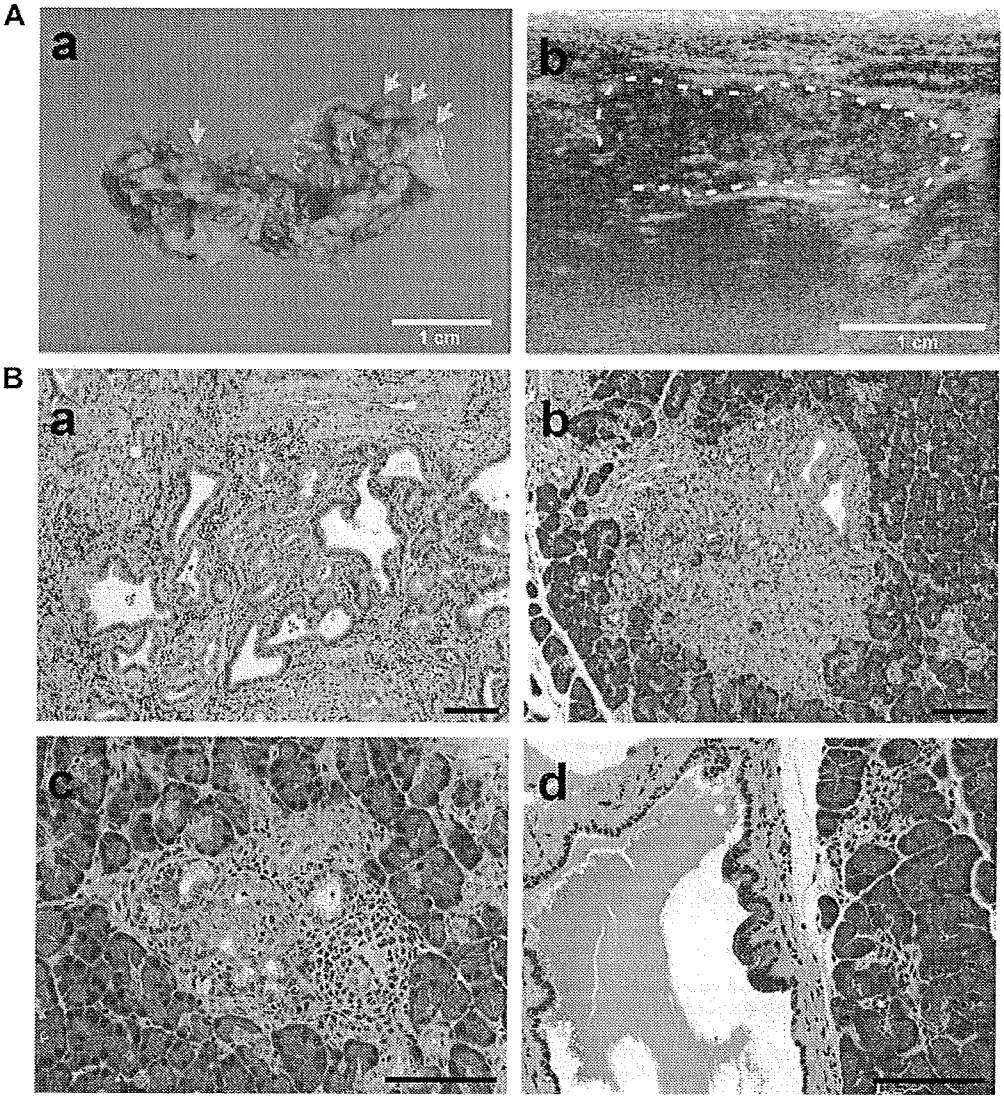

Fig. 1. Pancreas tumors developed in *ras* Tg rats. Animals were killed 3–4 weeks after injection of recombinant AxCANCre into the pancreas of adult *ras* Tg rats. (A) Macroscopic appearance of the pancreas with advanced multiple tumors (arrows) in an Hras250 rat (a). At this stage, multiple tumor nodules can be visualized by ultrasound image analysis (inside broken line) (b). (B) Histological appearance of pancreatic lesions. Large carcinoma (a), small carcinomas (b,c) and a PanIN-1a like lesion with slightly atypical duct epithelium (d). (a,b) are in Hras250 rats and (c) and (d) are grossly invisible small lesions in Kras327 rats. Bars = 100 μm.

Table 1
Microarray data: list of up-regulated genes encoding secreted proteins.

Gene	Accessions	Description	Expression level (tumor/control)
Mmp7	NM_012864	Matrix metalloproteinase-7	18.2
Tf	NM_001013110	Transferrin	14.4
Ctgf	NM_022266	Connective tissue growth factor	14.3
Cx3cl1	NM_134455	Chemokine (C-X3-C motif) ligand 1	7.7
Msln	NM_031658	Erc/Mesothelin	7.4
Lcn2	NM_130741	Lipocalin 2	7.0
Mmp2	U65656	Gelatinase A	6.0
Col18a1	XM_241632	Procollagen, type XVIII, alpha 1	5.5
Mgp	NM_012862	Matrix Gla protein	5.2
Sdc1	NM_013026	Syndecan 1	4.8

was determined using a rapid titer kit (Clontech, Mountain View, CA). Pancreas tumors were induced as described previously [4]. Ultrasound images were acquired using a microimaging system (EUB-8500, Hitachi Medical Corp., Tokyo, Japan). The pancreas was frozen in liquid nitrogen for RNA assays, or fixed in phosphate-buffered 10% formalin and processed for histological observation. Primary antibody anti-rat-C-ERC/Mesothelin (306) (IBL, Gunma, Japan) was used, and staining was performed using Vectastain ABC kits (Vector Laboratories, Burlingame, CA).

Tumors other than PDA were induced by chemical carcinogens, diethylnitrosamine (DEN) for liver cell tumor, *N*-butyl-*N*-(4-hydroxybutyl)nitrosamine (BBN) for bladder tumor, 7,12-dimethylbenz[a]anthracene (DMBA) for mammary tumor, *N*-bis(2-hydroxypropyl)nitrosamine (DHPN) for lung, kidney and thyroid tumor, and DMBA–12-*O*-tetradecanoylphorbol 13-acetate (TPA) for skin tumor.

Establishment of a rat pancreas cell line and Erc/Mesothelin analysis. A pancreas carcinoma cell line was established from a pancreas tumor from an Hras250 rat. The pancreas tumor tissue was placed in RPMI1640 medium at 4 °C. The tumor was diced into 1–2 mm^3 pieces and transplanted to NOD-SCID mice. Three months after transplantation, the tumor grew and reached a size of 10 mm in diameter. Tumor tissues were trimmed of fat and necrotic portions and minced with scalpels. The tissue pieces were transferred to 60-

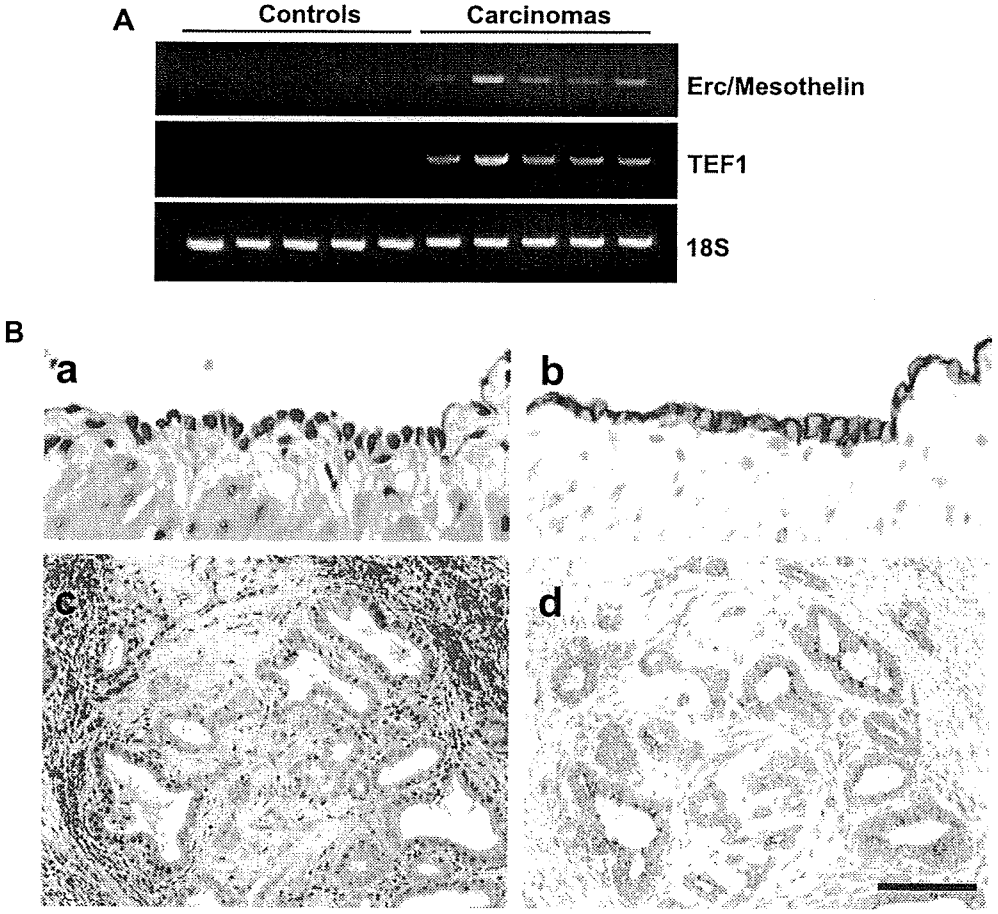

Fig. 2. Expression of Erc/Mesothelin in pancreatic lesions. (A) RT-PCR for Erc/Mesothelin and TEF-1 of normal pancreas and carcinomas in Hras250 rats. Each lane represent RNA prepared from an individual rat. 18S ribosome serves as an RNA control. (B) Immunostaining of Erc/Mesothelin in the mesothelium (a,b) and PDA (c,d) lesions. The antibody is more dense in the apical border. (a,c), H&E staining; (b,d), Erc/Mesothelin staining. Bar = 100 μm.

mm culture dishes at 10–15 fragments/dish. Fibroblasts were removed mechanically and by trypsinization (trypsin, 0.05%; EDTA, 0.02%). The cells were cultured on dishes. The established cell line was maintained in DMEM/Keratinocyte-SFM (Gibco, Grand Island, NY) containing 10% FCS. The cells were seeded in 1 ml of medium at a cell density of 10^5 cells/35-mm plate and cultured for 2 days. Cells were harvested and the cultured supernatant collected.

The tumor cells (1×10^6 or 1×10^7) were transplanted subcutaneously into 6 week old male NOD-SCID mice (Charles River Laboratories Japan, Inc., Yokohama, Japan). After 5 weeks of transplantation, the tumor was weighed and serum was collected for analysis of Erc/Mesothelin.

RT-PCR. Total RNA was isolated using ISOGEN (Nippon Gene, Toyama, Japan). A total of 450 ng of total RNA (from control pancreas and tumor samples) was reverse-transcribed using Superscript III Reverse Transcriptase with Random primers (Invitrogen, Carlsbad, CA). Reverse-transcription reaction mixtures were diluted 1:100 and 2 μl was used for PCR. The following primers were used: *Erc/Mesothelin*, 5′-ACCGTTGACTTTGCCAGTCT-3′ and 5′-TGCATCCGTCTCAC TCACTT-3′; *TEF-1*, 5′-ATTCTTACAGCGACCCGTTG-3′ and 5′-TGCTCCA TGCTCACTATTCG-3′; ribosome 18S, 5′-GTTGGTGGAGCGATTTGTCT-3′ and 5′-GGCCTCACTAAACCATCCAA-3′.

Serum test. The serum level of Erc/Mesothelin was quantified by the ELISA system (Code No.27765, Rat N-ERC/Mesothelin Assay Kit, IBL, Gunma, Japan) described previously [19]. Serum levels of CA19-9, Dupan-2, and SPan-1 were assayed by SRL, Inc. (Tokyo, Japan).

Microarray analysis. For gene microarray analysis, mRNA was isolated from total RNA (pooled sample from five animals) using a "Poly(A)+ Isolation Kit from total RNA" (Nippon Gene) according to the manufacturer's instructions. Microarray analysis was performed by Hokkaido System Science Co., Ltd. (Sapporo, Japan) using Whole Rat Oligo Microarray (Agilent Technologies, Inc., Santa Clara, CA). The experiments were performed twice by switching dyes reciprocally.

Results

Ras Tg rats, 10–30 weeks of age, were killed 3–4 weeks after injection of recombinant AxCANCre into the pancreatic duct via the common bile duct. Many grossly visible whitish tumor nodules were observed throughout the pancreas in both types of *ras* Tg rats, although they were slightly fewer in number in the Kras327 lines. Pancreas tumors developed in all *ras* Tg rats without any relationship to their age. These multiple tumors can be detected by ultrasound imaging (Fig. 1A). Histological examination showed that these nodules were adenocarcinomas with a variable amount of fibrotic tissue proliferation, some showing desmoplastic morphology. Neoplastic lesions were not found in any other organs. Carcinomas caused destruction of pancreas tissue by infiltrative growth, however, remote metastasis was not observed. Representative cases of an advanced carcinoma, early small carcinomas, and a PanIN-1a lesion are shown in Fig. 1B. These pancreas lesions were positive for alucian blue, cytokeratins 19 and 7, cyclooxigenase-2 (COX-2), matrix metalloproteinase-7 (MMP-7), epidermal growth factor (EGF) and EGFR, but negative for amylase, as reported previously [4].

Serum CA19-9, Dupan-2, and SPan-1, which are currently available serum markers for human pancreas cancer, were not detected in pancreas tumor-bearing rats using human antibodies. We performed a comprehensive and global analysis of over 40,000 genes to find diagnosis markers to detect rat PDA. Pancreas tumor tissue with frank ductal adenocarcinomas from Hras250 rats was subjected to microarray analysis. Table 1 lists the top 10 up-regulated genes encoding secreted proteins; secreted proteins are of particular interest for their potential diagnostic value. Our microarray analysis indicated that Erc/Mesothelin was overexpressed 7.4-fold in pancreas carcinoma tissue compared to pancreata of wild type littermates. Importantly, a previous report showed that overexpression of Erc/Mesothelin was identified in the majority of pancreas carcinomas in humans [15]. Therefore, we focused on the preferential expression of Erc/Mesothelin in PDA of *ras* Tg rats.

The expression level of the Erc/Mesothelin gene was confirmed by RT-PCR. Erc/Mesothelin gene expression in pancreatic carcinoma was higher than in the pancreata of wild type littermates (Fig. 2A). Recently, Hucl et al. reported that the presence of transcription enhancer factor (TEF)-1 was required for high cancer-specific expression of Erc/Mesothelin [21]. Similarly, we found that the mRNA expression level of TEF-1 was higher in pancreatic carcinomas than in pancreas tissue from wild type littermates (Fig. 2A). Finally, immunohistochemical studies showed higher expression of Erc/Mesothelin in small carcinoma lesions as compared to surrounding normal tissue (Fig. 2B).

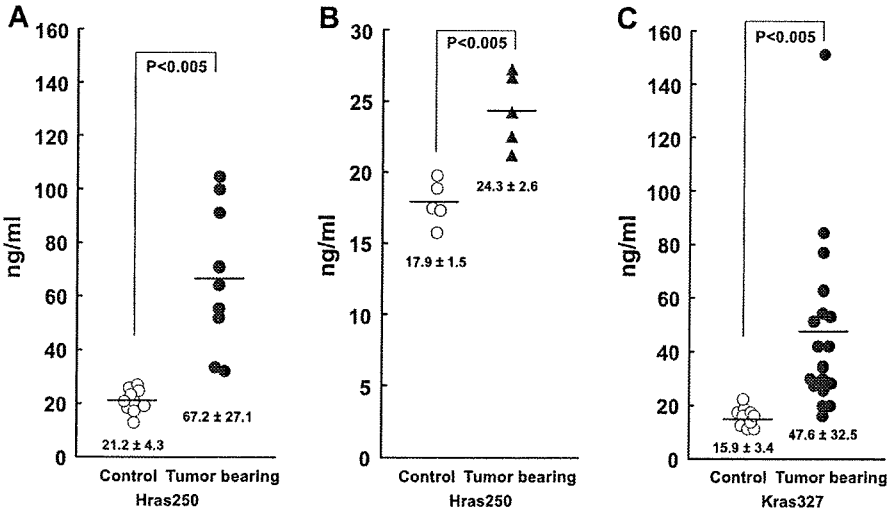

Fig. 3. Levels of N-ERC in rats bearing neoplastic lesions. (A) The serum levels of N-ERC in Hras250 rats bearing multiple pancreas ductal carcinomas was significantly higher than in untreated wild type control littermates ($P < 0.005$). (B) Serum N-ERC in Hras250 rats with early small carcinomas was also significantly higher than in untreated wild type control littermates ($P < 0.005$). The early lesions, not visible by eye, were detected microscopically. (C) The serum level of N-ERC in Kras327 rats bearing multiple pancreas ductal carcinomas was significantly higher than in untreated Kras327 control rats ($P < 0.005$). All animals were sacrificed 3 weeks after the AxCANCre injection.

We initially assayed the serum levels of the NH_2-terminal secretory form of Erc/Mesothelin (N-ERC) in Hras250 rats with pancreas carcinomas and in wild type littermates without pancreas carcinomas (Fig. 3). N-ERC levels in Hras250 rats bearing pancreas carcinomas was 67.2 ± 27.1 ng/ml (mean ± SD) (n = 9), whereas the levels in wild type Hras250 littermates was 21.2 ± 4.3 ng/ml (n = 10) (Fig. 3A). These results confirmed our ability to detect differences in serum N-ERC levels in animals in which Erc/Mesothelin was expressed at high (pancreas tumor-bearing Hras250 rats) and low (wild type littermates without pancreas tumors) levels.

To determine whether elevated levels of N-ERC can be detected in rats with early stage lesions, serum N-ERC levels in Hras250 rats with grossly normal-looking pancreas containing microscopic ductal adenoma/adenocarcinoma lesions were compared to untreated wild type littermates. The levels of N-ERC in rats with early lesions was 24.3 ± 2.6 ng/ml (n = 5) whereas the level in their untreated littermates was 17.9 ± 1.5 ng/ml (n = 5) (P < 0.005) (Fig. 3B). We then measured the levels of N-ERC in untreated Hras250 rats and in Hras250 rats treated with control adenovirus vector. The serum levels of N-ERC were the same in untreated Hras250 rats and Hras250 rats treated with control vector, and these levels were the same or somewhat lower than the levels in the Hras250 wild type littermates (data not shown). These results indicate that in the Hras250 animal model, increased N-ERC can be detected in the serum of animals with pre-malignant lesions.

Next we assayed N-ERC levels in the Kras transgenic rats. The level of N-ERC in tumor-bearing Kras327 rats was 47.6 ± 32.5 ng/ml (n = 18) whereas those of untreated Kras327 rats was 15.9 ± 3.4 ng/ml (n = 10) (P < 0.005) (Fig. 3C). In all serum samples, the COOH-terminal form of Erc/Mesothelin (C-ERC) was undetectable.

Since PDA lesions frequently include variable amounts of mesenchymal tissue, an increase in tumor associated mesothelial cells could cause an increase in serum N-ERC levels. We therefore evaluated the levels in a pancreas carcinoma cell line (designated 634NOD) derived from a pancreas ductal adenocarcinoma from an Hras250 rat. 634NOD cells were implanted subcutaneously into the flank of NOD-SCID mice, and the resulting tumor was positive for cytokeratins 19 and 7, markers of pancreatic duct (histology not shown). In tissue culture, the 634NOD cells expressed Erc/Mesothelin (Fig. 4A), and N-ERC could be detected in the culture supernate (389.4 ± 11.7 ng/ml) (Fig. 4B). C-ERC levels were extremely low to undetectable (Fig. 4B). Taken together, the results reported here clearly indicate that the elevated N-ERC detected in the serum of transgenic rats bearing pre-malignant pancreatic lesions was derived from these lesions.

To determine whether serum levels of N-ERC correlated with tumor size, we assayed N-ERC levels in NOD-SCID mice with transplanted 634NOD cells. N-ERC was detected in the serum of these mice. Increase in the serum level of N-ERC correlated with increased with tumor size (R = 0.918, P < 0.001) (Fig. 4C). This result indicates a causal relationships between serum level of N-ERC and tumor size.

Serum N-ERC levels in rats with tumors such as bladder transitional cell tumors, liver cell tumors, lung, kidney, thyroid, mammary, prostate, and skin tumors induced by chemical carcinogens were not significantly elevated compared to their respective controls (data not shown).

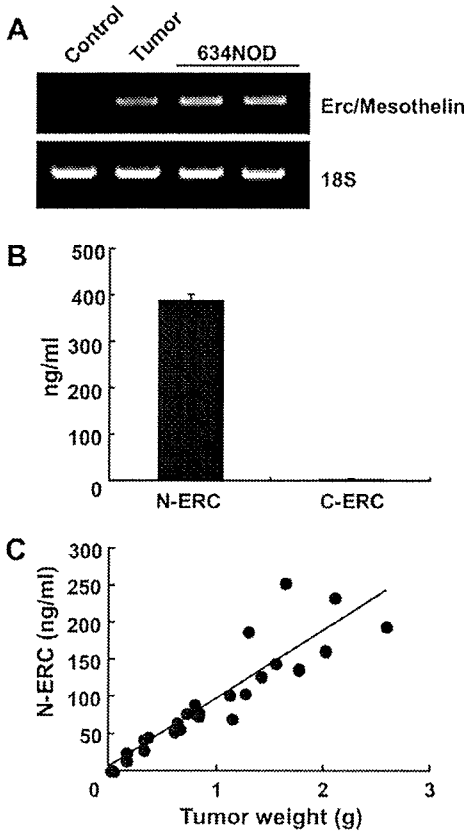

Fig. 4. The Erc/Mesothelin gene was expressed in an established pancreas ductal carcinoma cell line. (A) RT-PCR for Erc/Mesothelin in a pancreas carcinoma cell line. Control: pancreas from empty vector treated Hras250 rats (pooled sample from five animals). Tumor: pancreas carcinomas from AxCANCre injected Hras250 rats (pooled sample from five animals). 634NOD: pancreas carcinoma cell line (established from a pancreas tumor from an AxCANCre injected Hras250 rat). (B) Levels of N- and C-terminal derived Erc/Mesothelin (N-ERC and C-ERC, respectively) protein in the culture medium from a pancreas carcinoma cell line. The precursor protein is cleaved by a furin-like protease: a 31 kDa NH_2-terminal half (N-ERC) is released into the extracellular space, leaving the 40 kDa COOH-terminal half (Mesothelin) attached to the cell surface by a GPI-anchor. (C) Serum level of N-ERC in 634NOD transplanted NOD-SCID mice. The serum level of N-ERC correlated with increased tumor weight (R = 0.918, P < 0.001).

Discussion

For the purpose of developing methods to detect early cancer lesions, preferably at a preclinical stage, use of an appropriate animal model is advantageous because of the experimental availability of early lesions. To the best of our knowledge, available serum markers for cancer in animal models are limited to prostate cancer [22]. Antibodies for pancreas tumor associated human serum markers CA19-9, Dupan-2 and SPan-1 recognize carbohydrate chains, such as Sialyl Le^a, Sialyl Le^c. In this study, we found that serum levels of CA19-9, Dupan-2, and SPan-1 were below detectable levels in pancreas tumor-bearing rats regardless of stage. Cross-reactivity of these antibodies for human tumor carbohydrate antigen in rodents has not been clearly demonstrated. We have established rat models of pancreas ductal carcinomas. These models use a human $Hras^{G12V}$ (Hras250) [4] or a human $Kras^{G12V}$ (Kras327) oncogene under the control of the Cre/loxP system to induce cancerous lesions. Neoplastic lesions in the *ras* Tg rats exhibited morphological and biological similarities to those observed in human pancreas lesions. Using these models, we showed that preclinical pancreas ductal neoplasms can be diagnosed by measuring Erc/Mesothelin in the serum (Fig. 3).

N-ERC is a 31 kDa protein that forms the N-terminal fragment of the full-length 71 kDa Erc/Mesothelin protein and is secreted into the blood of mesothelioma patients. The ELISA system used in this study was originally used for the detection of N-ERC in the serum of mesothelioma patients [16]. The system was also used to detect N-ERC in the serum of Eker rats [18,23,24], and it

clearly worked in this study to detect higher levels of N-ERC in the serum of pancreas tumor-bearing rats. The expression levels of TEF-1 mRNA in pancreas tumors correlated with that of Erc/Mesothelin in tumor tissue and N-ERC in the serum. Since Erc/Mesothelin mRNA was found at relatively low levels in the normal rat pancreas, increased serum levels of N-ERC appear to be specific for pancreas carcinomas in the *ras* Tg rat models.

Many human pancreas cancer cell lines express Erc/Mesothelin [12,21,25]. N-ERC was detected in the supernatants of cultured human pancreas cancer cells, and correlated with the expression levels of Erc/Mesothelin [25]. Although there was no significant difference in serum N-ERC concentrations between pancreas cancer patients and healthy control groups [25], Erc/Mesothelin is frequently expressed in ductal carcinoma, but not in normal pancreas or chronic pancreatitis [15,25–27]. Thus, Erc/Mesothelin expression can be found in both human and rat pancreas ductal adenocarcinoma.

Previous immunohistochemical studies showed that expression of Mesothelin is found in most epithelioid mesothelioma, nonmucinous carcinomas of the ovary, adenocarcinomas of the pancreas, some breast, uterus, colorectal and lung adenocarcinomas, but not in carcinomas of the prostate, kidney, liver, thyroid, or bladder in humans [13,27–29]. In line with human data, although we have not thoroughly examined all the different tumors induced by chemical carcinogens, available data indicates that increase in serum N-ERC level is relatively specific for PDA in rats.

One advantage of using rats is that their relatively large organ size facilitates surgical procedures. In this rat model, serum levels of N-ERC can be used for the identification of early neoplastic lesions, even in preclinical stages, and also for monitoring the further progression of carcinogenesis. The model may also be used to screen for candidate chemotherapeutic agents, which could be evaluated for human use. Furthermore, serum N-ERC may prove useful for the diagnosis of pre-symptomatic lesions for human mesothelioma or ovary cancer patients.

Acknowledgments

We thank Dr. T. Sugimura (National Cancer Center) for his valuable advice, Dr. T. Shirai (Nagoya City University) for his assistance with histological specimen preparation and advice for histological examination, Drs. M. Wei (Osaka City University), S. Tamano (DIMS institute of Medical Science), S. Yamashita and T. Ushijima (National Cancer Center) for rat serum provision, and Dr. J. Miyazaki (Osaka University) for the CAG promoter provision. We also thank Y. Morita, S. Ariji, K. Ohmi and Y. Terashima, training students, for their enthusiastic assistance with establishment of the transgenic rats.

This work was supported in part by the Grant-in-Aid for Scientific Research (C) from Japan Society for the Promotion of Science, the Grant-in-Aid for Cancer Research (15-2, 16-13, 17S-6, 20S-8), the Grant-in-Aid for Research on Nanotechnical Medical (H19-nano-ippan-014), the Grant-in-Aid for Research on Risk of Chemical Substances (H18-kagaku-ippan-007, H19-Kagaku-Ippan-006) from the Ministry of Health, Labour, and Welfare of Japan, and Grant-in-Aid for Food Safety Commission, Japan (051).

References

[1] H.G. Beger, B. Rau, F. Gansauge, B. Poch, K.H. Link, Treatment of pancreatic cancer: challenge of the facts, World J. Surg. 27 (2003) 1075–1084.
[2] A. Jemal, R. Siegel, E. Ward, T. Murray, J. Xu, M.J. Thun, Cancer statistics, 2007, CA Cancer J. Clin. 57 (2007) 43–66.
[3] E.P. DiMagno, H.A. Reber, M.A. Tempero, AGA technical review on the epidemiology, diagnosis, and treatment of pancreatic ductal adenocarcinoma, Am. Gastroenterol. Assoc. Gastroenterol. 117 (1999) 1464–1484.
[4] S. Ueda, K. Fukamachi, Y. Matsuoka, N. Takasuka, F. Takeshita, A. Naito, M. Iigo, D.B. Alexander, M.A. Moore, I. Saito, T. Ochiya, H. Tsuda, Ductal origin of pancreatic adenocarcinomas induced by conditional activation of a human Ha-ras oncogene in rat pancreas, Carcinogenesis 27 (2006) 2497–2510.
[5] O. Hino, E. Kobayashi, M. Nishizawa, Y. Kubo, T. Kobayashi, Y. Hirayama, S. Takai, Y. Kikuchi, H. Tsuchiya, K. Orimoto, K. Kajino, T. Takahara, H. Mitani, Renal carcinogenesis in the Eker rat, J. Cancer Res. Clin. Oncol. 121 (1995) 602–605.
[6] Y. Yamashita, M. Yokoyama, E. Kobayashi, S. Takai, O. Hino, Mapping and determination of the cDNA sequence of the Erc gene preferentially expressed in renal cell carcinoma in the Tsc2 gene mutant (Eker) rat model, Biochem. Biophys. Res. Commun. 275 (2000) 134–140.
[7] K. Chang, I. Pastan, Molecular cloning of mesothelin, a differentiation antigen present on mesothelium, mesotheliomas, and ovarian cancers, Proc. Natl. Acad. Sci. USA 93 (1996) 136–140.
[8] T. Kojima, M. Oh-eda, K. Hattori, Y. Taniguchi, M. Tamura, N. Ochi, N. Yamaguchi, Molecular cloning and expression of megakaryocyte potentiating factor cDNA, J. Biol. Chem. 270 (1995) 21984–21990.
[9] K. Chang, L.H. Pai, J.K. Batra, I. Pastan, M.C. Willingham, Characterization of the antigen (CAK1) recognized by monoclonal antibody K1 present on ovarian cancers and normal mesothelium, Cancer Res. 52 (1992) 181–186.
[10] K. Chang, I. Pastan, M.C. Willingham, Isolation and characterization of a monoclonal antibody, K1, reactive with ovarian cancers and normal mesothelium, Int. J. Cancer 50 (1992) 373–381.
[11] K. Chang, I. Pastan, Molecular cloning and expression of a cDNA encoding a protein detected by the K1 antibody from an ovarian carcinoma (OVCAR-3) cell line, Int. J. Cancer 57 (1994) 90–97.
[12] N. Yamaguchi, K. Hattori, M. Oh-eda, T. Kojima, N. Imai, N. Ochi, A novel cytokine exhibiting megakaryocyte potentiating activity from a human pancreatic tumor cell line HPC-Y5, J. Biol. Chem. 269 (1994) 805–808.
[13] N. Scholler, N. Fu, Y. Yang, Z. Ye, G.E. Goodman, K.E. Hellstrom, I. Hellstrom, Soluble member(s) of the mesothelin/megakaryocyte potentiating factor family are detectable in sera from patients with ovarian carcinoma, Proc. Natl. Acad. Sci. USA 96 (1999) 11531–11536.
[14] C.D. Hough, C.A. Sherman-Baust, E.S. Pizer, F.J. Montz, D.D. Im, N.B. Rosenshein, K.R. Cho, G.J. Riggins, P.J. Morin, Large-scale serial analysis of gene expression reveals genes differentially expressed in ovarian cancer, Cancer Res. 60 (2000) 6281–6287.
[15] P. Argani, C. Iacobuzio-Donahue, B. Ryu, C. Rosty, M. Goggins, R.E. Wilentz, S.R. Murugesan, S.D. Leach, E. Jaffee, C.J. Yeo, J.L. Cameron, S.E. Kern, R.H. Hruban, Mesothelin is overexpressed in the vast majority of ductal adenocarcinomas of the pancreas: identification of a new pancreatic cancer marker by serial analysis of gene expression (SAGE), Clin. Cancer Res. 7 (2001) 3862–3868.
[16] K. Shiomi, H. Miyamoto, T. Segawa, Y. Hagiwara, A. Ota, M. Maeda, K. Takahashi, K. Masuda, Y. Sakao, O. Hino, Novel ELISA system for detection of N-ERC/mesothelin in the sera of mesothelioma patients, Cancer Sci. 97 (2006) 928–932.
[17] K. Shiomi, Y. Hagiwara, K. Sonoue, T. Segawa, K. Miyashita, M. Maeda, H. Izumi, K. Masuda, M. Hirabayashi, T. Moroboshi, T. Yoshiyama, A. Ishida, Y. Natori, A. Inoue, M. Kobayashi, Y. Sakao, H. Miyamoto, K. Takahashi, O. Hino, Sensitive and specific new enzyme-linked immunosorbent assay for N-ERC/Mesothelin increases its potential as a useful serum tumor marker for mesothelioma, Clin. Cancer Res. 14 (2008) 1431–1437.
[18] M. Nakaishi, K. Kajino, M. Ikesue, Y. Hagiwara, M. Kuwahara, H. Mitani, Y. Horikoshi-Sakuraba, T. Segawa, S. Kon, M. Maeda, T. Wang, M. Abe, M. Yokoyama, O. Hino, Establishment of the enzyme-linked immunosorbent assay system to detect the amino terminal secretory form of rat Erc/Mesothelin, Cancer Sci. 98 (2007) 659–664.
[19] Y. Hagiwara, Y. Hamada, M. Kuwahara, M. Maeda, T. Segawa, K. Ishikawa, O. Hino, Establishment of a novel specific ELISA system for rat N- and C-ERC/mesothelin. Rat ERC/mesothelin in the body fluids of mice bearing mesothelioma, Cancer Sci. 99 (2008) 666–670.
[20] M. Asamoto, T. Ochiya, H. Toriyama-Baba, T. Ota, T. Sekiya, M. Terada, H. Tsuda, Transgenic rats carrying human c-Ha-ras proto-oncogenes are highly susceptible to *N*-methyl-*N*-nitrosourea mammary carcinogenesis, Carcinogenesis 21 (2000) 243–249.
[21] T. Hucl, J.R. Brody, E. Gallmeier, C.A. Iacobuzio-Donahue, I.K. Farrance, S.E. Kern, High cancer-specific expression of mesothelin (MSLN) is attributable to an upstream enhancer containing a transcription enhancer factor dependent MCAT motif, Cancer Res. 67 (2007) 9055–9065.
[22] I.V. Huizen, G. Wu, M. Moussa, J.L. Chin, A. Fenster, J.C. Lacefield, H. Sakai, N.M. Greenberg, J.W. Xuan, Establishment of a serum tumor marker for preclinical trials of mouse prostate cancer models, Clin. Cancer Res. 11 (2005) 7911–7919.
[23] O. Hino, Multistep renal carcinogenesis in the Eker (Tsc 2 gene mutant) rat model, Curr. Mol. Med. 4 (2004) 807–811.
[24] M. Maeda, O. Hino, Molecular tumor markers for asbestos-related mesothelioma: serum diagnostic markers, Pathol. Int. 56 (2006) 649–654.
[25] K. Inami, K. Kajino, M. Abe, Y. Hagiwara, M. Maeda, M. Suyama, S. Watanabe, O. Hino, Secretion of N-ERC/mesothelin and expression of C-ERC/mesothelin in human pancreatic ductal carcinoma, Oncol. Rep. 20 (2008) 1375–1380.
[26] R. Hassan, Z.G. Laszik, M. Lerner, M. Raffeld, R. Postier, D. Brackett, Mesothelin is overexpressed in pancreaticobiliary adenocarcinomas but not in normal pancreas and chronic pancreatitis, Am. J. Clin. Pathol. 124 (2005) 838–845.
[27] N.G. Ordonez, Application of mesothelin immunostaining in tumor diagnosis, Am. J. Surg. Pathol. 27 (2003) 1418–1428.
[28] N.G. Ordonez, Value of mesothelin immunostaining in the diagnosis of mesothelioma, Mod. Pathol. 16 (2003) 192–197.
[29] H.F. Frierson Jr., C.A. Moskaluk, S.M. Powell, H. Zhang, L.A. Cerilli, M.H. Stoler, H. Cathro, G.M. Hampton, Large-scale molecular and tissue microarray analysis of mesothelin expression in common human carcinomas, Hum. Pathol. 34 (2003) 605–609.

Stress-Activated Mitogen-Activated Protein Kinases c-Jun NH_2-Terminal Kinase and p38 Target Cdc25B for Degradation

Sanae Uchida,[1,2] Katsuji Yoshioka,[3] Ryoichi Kizu,[4] Hitoshi Nakagama,[5] Tsukasa Matsunaga,[1] Yukihito Ishizaka,[6] Randy Y.C. Poon,[7] and Katsumi Yamashita[1]

[1]Division of Life Science, Graduate School of Natural Science and Technology, [2]Venture Business Laboratory, Center for Innovation, and [3]Division of Molecular Cell Signaling, Cancer Research Institute, Kanazawa University, Kanazawa, Japan; [4]Laboratory of Environmental Biochemistry, Faculty of Pharmaceutical Science, Doshisha Women's College of Liberal Arts, Kyotanabe, Japan; [5]Division of Biochemistry, National Cancer Center Research Institute; [6]Division of Intractable Diseases, Research Institute, International Medical Center of Japan, Tokyo, Japan; and [7]Department of Biochemistry, Hong Kong University of Science and Technology, Clear Water Bay, Hong Kong

Abstract

Cdc25 dual specificity phosphatases positively regulate the cell cycle by activating cyclin-dependent kinase/cyclin complexes. Of the three mammalian Cdc25 isoforms, Cdc25A is phosphorylated by genotoxic stress–activated Chk1 or Chk2, which triggers its $SCF^{\beta\text{-}TrCP}$–mediated degradation. However, the roles of Cdc25B and Cdc25C in cell stress checkpoints remain inconclusive. We herein report that c-Jun NH_2-terminal kinase (JNK) induces the degradation of Cdc25B. Nongenotoxic stress induced by anisomycin caused rapid degradation of Cdc25B as well as Cdc25A. Cdc25B degradation was dependent mainly on JNK and partially on p38 mitogen-activated protein kinase (p38). Accordingly, cotransfection with JNK1, JNK2, or p38 destabilized Cdc25B. *In vitro* kinase assays and site-directed mutagenesis experiments revealed that the critical JNK and p38 phosphorylation site in Cdc25B was Ser^{101}. Cdc25B with Ser^{101} mutated to alanine was refractory to anisomycin-induced degradation, and cells expressing such mutant Cdc25B proteins were able to override the anisomycin-induced G_2 arrest. These results highlight the importance of a novel JNK/p38-Cdc25B axis for a nongenotoxic stress–induced cell cycle checkpoint. [Cancer Res 2009;69(16):6438–44]

Introduction

Cell cycle progression in eukaryotic cells requires the successive activation and inactivation of cyclin-dependent kinase (CDK)-cyclin complexes. Activation of CDK-cyclin complexes depends on members of the Cdc25 dual specificity phosphatases. In mammalian cells, the Cdc25 family consists of Cdc25A, Cdc25B, and Cdc25C. Although Cdc25C was the first member to be identified, Cdc25A is now regarded as one of the major players in multiple phases of cell cycle progression in mammalian somatic cells (1, 2). Besides its well-known role in G_1-S transition, Cdc25A is also involved in the G_2-M transition and chromosome condensation (1, 3, 4). Moreover, Cdc25A is also a well-known target of the DNA damage checkpoint (2, 5). On genotoxic insults, Cdc25A is rapidly phosphorylated by the checkpoint kinases Chk1 and Chk2 followed by $SCF^{\beta\text{-}TrCP}$–mediated ubiquitinylation and degradation (2, 6).

In contrast to Cdc25A, the roles of Cdc25B and Cdc25C remain elusive. Experiments with Cdc25B- or Cdc25C-knockout mice indicate that these genes are dispensable not only for normal cell cycle control but also for the DNA damage checkpoint (7, 8). The only prominent phenotype is a defect in oocyte maturation in Cdc25B-depleted female mice (9). However, several lines of evidence suggest that Cdc25B is important for controlling CDK1-cyclin B activity at the centrosome, where the kinase contributes to centrosome separation at prophase (4, 10). Chk1 is believed to down-regulate the activity of Cdc25B until prophase (11, 12). The phosphorylation of Cdc25B (Ser^{309} of Cdc25B1 or Ser^{323} in Cdc25B3) has also been implicated in the function of Cdc25B in conjunction with 14-3-3 binding (13, 14). A mutation that abolishes the specific phosphorylation site causes Cdc25B to localize to the nucleus and enhances its ability to abrogate DNA damage–induced G_2 arrest (15, 16). These results suggest that despite its nonessentiality in mouse models, Cdc25B does play some role in the G_2-M transition (14).

Stress stimuli that do not target genome DNA lead to the activation of the so-called stress-activated mitogen-activated protein kinases (MAPK), including p38 MAPK (p38) and c-Jun NH_2-terminal kinase (JNK; ref. 17). Recently, MAPKAP kinase 2 (MK2) has received attention for its ability to phosphorylate Cdc25B, leading to 14-3-3 binding (18). MK2 is usually complexed with and activated by p38 (18). Therefore, a fraction of p38 can be found to coimmunoprecipitate with MK2, which could mislead one to believe that p38 phosphorylates substrates that are normally phosphorylated exclusively by MK2. The p38-MK2 cascade is, therefore, believed to regulate cell cycle progression by controlling the stability and subcellular localization of Cdc25A and Cdc25B, respectively, when cells are exposed to genotoxic or nongenotoxic stress (14, 18–20). JNK also phosphorylates and inactivates Cdc25C (21). In addition, nuclear Cdc25B is exported to the cytoplasm on UV or nongenotoxic stress by an unknown mechanism (22).

We previously reported that overexpression of 14-3-3 causes the relocation of Cdc25B from the nucleus to the cytoplasm (13, 23, 24). To delineate the role of the cytoplasmic export of Cdc25B, we established HeLa cell lines that constitutively express Cdc25B and investigated conditions that induce nuclear export of the phosphatase. We found that nongenotoxic stress, but not genotoxic cell stress, induced loss of Cdc25B nuclear localization and that nongenotoxic stress was also an effective inducer of Cdc25B degradation. Moreover, we found that the stability of Cdc25B could be controlled by JNK and p38. These data reveal a novel pathway linking the stress response kinases to the G_2-M cell cycle engine.

Materials and Methods

Reagents, plasmids, and antibodies. Reagents of the highest grade were obtained from Wako or Sigma. Restriction enzymes were obtained from New England Biolabs, and MKK7-activated recombinant JNK1 and

Note: Supplementary data for this article are available at Cancer Research Online (http://cancerres.aacrjournals.org/).

Requests for reprints: Katsumi Yamashita, Division of Life Sciences, Graduate School of Natural Science and Technology, Kanazawa University, Kakuma-machi, Kanazawa 920-1192, Ishikawa, Japan. Phone: 81-76-264-6270; Fax: 81-76-264-6270; E-mail: katsumi@kenroku.kanazawa-u.ac.jp.

doi:10.1158/0008-5472.CAN-09-0869

MKK6-activated p38α (both isolated from baculovirus-infected Sf21 cells) were obtained from Upstate. Oligonucleotides were synthesized by Invitrogen. The cDNAs and antibodies used in the experiments were described in Supplementary Materials and Methods.

Cell culture and plasmid transfection. HeLa cells were grown in DMEM as previously described (13). Plasmids were transiently transfected with Lipofectamine 2000 (Invitrogen). Cell cycle synchronization was performed using the double thymidine block protocol. To obtain stable Flag-tagged Cdc25B (F-Cdc25B)–expressing HeLa cells, we used 10 μg/mL blasticidin S (Invitrogen) for the selection of transformed cells. Established Flag-Cdc25B–expressing HeLa cells were maintained with 2 μg/mL blasticidin S.

Preparation of crude extracts, immunoblotting, immunoprecipitation, and kinase assay. Crude extracts for the analysis of proteins followed by immunoblotting or immunoprecipitation were performed as described previously (13). To detect endogenous Cdc25B, we subjected proteins that had been immunoprecipitated with rabbit anti-Cdc25B antibodies to SDS-PAGE, followed by immunoblotting. The Cdc25B protein was detected with mouse monoclonal anti-Cdc25B antibody. The immunoprecipitates used for the kinase assay were washed twice with buffer containing 100 mmol/L Tris-HCl (pH 8.0), 5 mmol/L EGTA, and 20 mmol/L $MgCl_2$. The samples were then incubated with the same buffer that was supplemented with appropriate glutathione *S*-transferase (GST) fusion Cdc25B proteins, 1 mmol/L DTT, 200 μmol/L ATP, and [γ-^{32}P]ATP (1 μCi = 37 KBq; Perkin-Elmer). The reaction mixtures were incubated at 30°C for 60 min and subjected to SDS-PAGE, and radioactivity was detected using the Fuji BAS system (Fujifilm).

Indirect immunofluorescence and flow cytometry. Indirect immunofluorescence of cells grown on glass coverslips was conducted as described previously (13). Cells treated for fluorescence-activated cell sorting (FACS) were analyzed on a FACSCalibur (BD Biosciences) using ModFit software. The Ser^{10}-phosphorylated histone H3 (phospho-S10-H3)–positive cells were analyzed using CellQuest software.

Results

Nuclear localization of Cdc25B is lost following treatment of cells with anisomycin but not with DNA-damaging agents. Phosphorylation of Ser^{309} of Cdc25B1 followed by binding of 14-3-3 disrupts nuclear localization of Cdc25B (13). Ser^{309} can be phosphorylated by Chk1/2 and MK2 (18, 25, 26). To determine the types of cellular stresses that induce nuclear export, we treated cells with various chemicals and analyzed the subcellular localization of Cdc25B. Given that an antibody that displayed high specificity toward endogenous Cdc25B was not available commercially or in house, we first established a HeLa cell–based cell line that constitutively expressed F-Cdc25B. No gross abnormality of cell growth or morphology was discerned for F-Cdc25B–expressing cells, which are hereafter called HeLa-W40 cells.

We treated HeLa-W40 cells with hydroxyurea, aphidicolin, etoposide, or camptothecin, which activate either Chk1 or Chk2. DNA damage induced by the chemicals was confirmed by assaying for phosphorylated histone H2AX (γ-H2AX; ref. 27). Cdc25B localized to the nucleus in cells with or without DNA damage or replication arrest (Fig. 1*A*). We next investigated the possible involvement of the p38/MK2 pathways in this process. To activate the p38/MK2 pathway, we treated the cells with anisomycin, which activates p38 and JNK (28, 29). Treatment with anisomycin disrupted the nuclear localization of Cdc25B and promoted the redistribution of Cdc25B to the cytoplasm (Fig. 1*B*). These results suggest that Cdc25B nuclear localization can be disrupted by stress pathways other than those initiated by DNA damage.

To assess the possibility that the p38 pathway regulates Cdc25B, we added the p38 inhibitor SB202190 to HeLa-W40 cells. Of interest

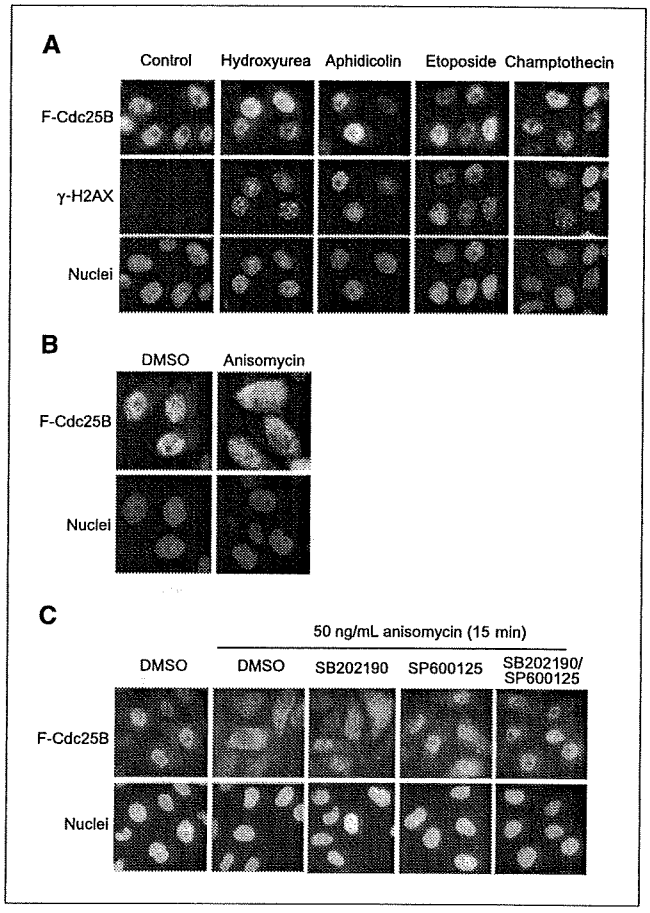

Figure 1. Nuclear localization of Cdc25B is maintained after DNA damage but is disturbed by anisomycin treatment. *A*, HeLa-W40 cells were treated with the indicated chemicals and Flag-Cdc25B and γ-H2AX were detected by indirect immunofluorescence. The nuclei were identified using 4′,6-diamidino-2-phenylindole. The conditions for chemical treatment were described in Supplementary Materials and Methods. *B*, HeLa-W40 cells were treated with 50 ng/mL anisomycin for 15 min and processed for indirect immunofluorescence. *C*, HeLa-W40 cells were pretreated with the indicated MAPK inhibitors for 1 h followed by anisomycin challenge. The cells were fixed, and Flag-Cdc25B and nuclei were analyzed. The concentration for inhibitors was as follows: SB202190, 20 μmol/L; SP600125, 20 μmol/L.

is that SB202190 exerted only a small effect on the anisomycin-induced diffusion of Cdc25B (Fig. 1*C*). In contrast, the JNK inhibitor SP600125 induced strong nuclear staining of Cdc25B under conditions of anisomycin stress. Furthermore, stronger nuclear signals for Cdc25B were generated by simultaneous treatment with both SB202190 and SP600125 than by treatment with SP600125 alone. Inhibition of MAPK/extracellular signal-regulated kinase (ERK) kinase (MEK1) with U0126, thereby inhibiting the activation of ERK1/2, did not prevent cytoplasmic diffusion of Cdc25B (data not shown). Collectively, these data indicate that anisomycin-mediated stress can disrupt nuclear localization of Cdc25B in a JNK-dependent manner.

Cdc25B is degraded in cells treated with anisomycin or sodium chloride but not with DNA-damaging agents. The signals for F-Cdc25B faded in cells after long-term exposure to anisomycin but not after treatment with DNA-damaging agents (data not shown). These observations led us to analyze the level of F-Cdc25B protein in HeLa-W40 cells treated with anisomycin and another

nongenotoxic reagent, sodium chloride (NaCl). We also examined the levels of Cdc25A and Cdc25C to determine whether different cellular stresses affect members of this phosphatase family. Genotoxic stress caused by exposure to hydroxyurea, aphidicolin, etoposide, or camptothecin effectively induced Cdc25A degradation (Fig. 2*A*). In contrast, expression of Cdc25B or Cdc25C was unaffected under the same conditions. Although neither anisomycin nor NaCl activated Chk1 or Chk2, both Cdc25B and Cdc25A were degraded (Fig. 2*A*). Cdc25A and Cdc25B decreased in a time-dependent fashion after exposure to anisomycin (Fig. 2*B*). The endogenous Cdc25B protein in parental HeLa cells was also degraded by anisomycin treatment but not by DNA-damaging agents (Supplementary Fig. S1). The abundance of Cdc25C was not affected by any of the stimuli examined here. UV irradiation, which is known to activate not only Chk1/2 but also p38/JNK, abrogated nuclear localization of Cdc25B as reported (22) and induced Cdc25B degradation (Supplementary Fig. S2*A* and *B*).

Although anisomycin inhibits protein synthesis (29), the more rapid decline of Cdc25B in anisomycin-treated cells compared with cycloheximide-treated cells suggested that degradation of Cdc25B was specifically caused by anisomycin-induced stress and not by a general inhibition of protein synthesis (Fig. 2*C*). More convincing evidence was obtained when we examined the stability of Cdc25B that contained mutations at the constitutive β-TrCP binding site of ^{254}DDGFVD^{259} (amino acid numbering is based on human Cdc25B1; ref. 30). The site is responsible for the steady-state degradation of Cdc25B by a constitutive SCF$^{\beta\text{-TrCP}}$–mediated ubiquitin-proteasome pathway. We established a HeLa cell line expressing a mutant Cdc25B that contained mutations at the β-TrCP binding site (Cdc25B^{DAA}, of which D255 and G256 were replaced by Ala). Figure 2*D* shows that Cdc25B^{DAA} was unstable after anisomycin treatment. This indicates that the Cdc25B degradation was specific to anisomycin treatment. Collectively, these data indicate that anisomycin-induced stress, but not DNA damage–induced stress, triggers a loss of nuclear localization and stability of Cdc25B.

Inhibition of JNK attenuates the degradation of Cdc25B by anisomycin. To determine the role of p38 or JNK on the stability of Cdc25A and Cdc25B, we treated HeLa cells with inhibitors of p38 or JNK and analyzed the cellular proteins. The activation of p38α/β was monitored as the slower migrating form of MK2, corresponding to phosphorylated MK2 (Fig. 3*A*); JNK activation was monitored using antibodies recognizing phospho-JNK1 or phospho–c-Jun. We found that the JNK inhibitor SP600125 protected Cdc25B from anisomycin-induced degradation (Fig. 3*A*, *lanes 5–8*). A relatively small but definite contribution of the p38 pathway to the degradation of Cdc25B was revealed by these experiments (Fig. 3*A*, *lanes 3–8*). The MEK1 inhibitor U0126 again had no effect on the stability of either Cdc25A or Cdc25B (data not shown). Time course experiments further validated the critical role of JNK in regulating the degradation of Cdc25B (Fig. 3*B*). The stability of Cdc25C was essentially unaffected by these inhibitors (Fig. 3*A*). Exactly the same results were obtained with HeLa-W40 cells that expressed F-Cdc25B (Supplementary Fig. S3*A*). JNK inhibitor also attenuated the NaCl-induced F-Cdc25B degradation (Supplementary Fig. S3*B*). Results shown in Fig. 3*C* indicate the correlation between the degradation of Cdc25A/Cdc25B and activation of p38/JNK. Anisomycin-, NaCl-, or UV-induced degradation of Cdc25B was inhibited by the proteasome inhibitor MG132, suggesting that the anisomycin-induced degradation of Cdc25B is mediated by the ubiquitin-proteasome pathway (Supplementary Fig. S3*C*, *1*, *2*, and *3*).

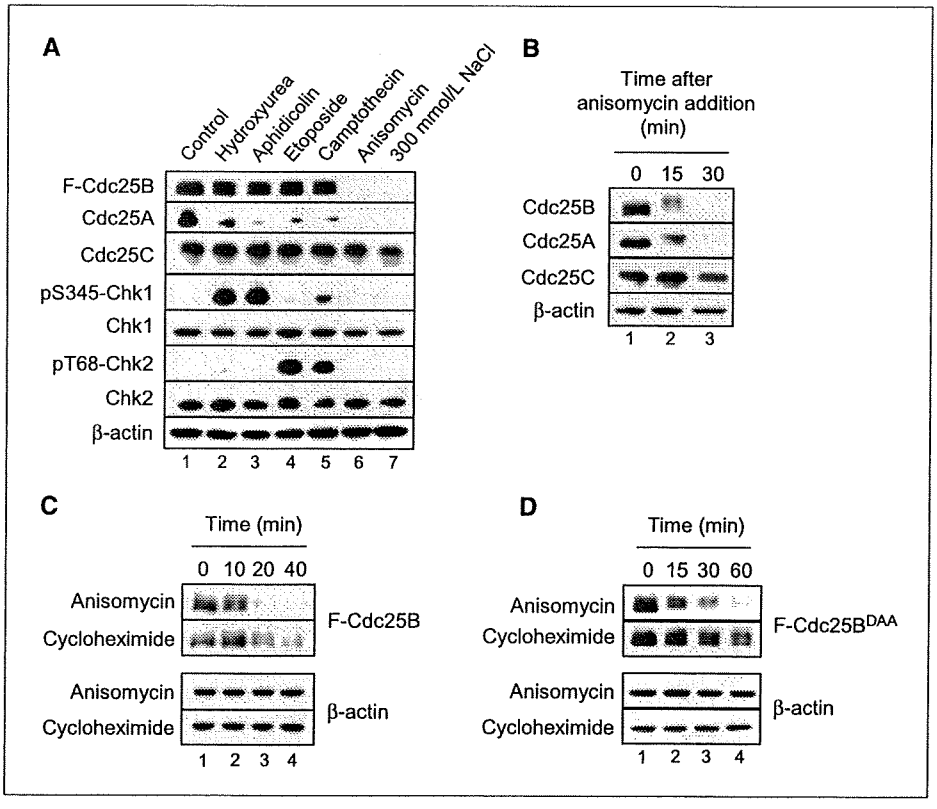

Figure 2. Degradation of Cdc25A and Cdc25B after treatment with DNA-damaging or non–DNA-damaging agents. *A*, HeLa-W40 cells were treated with genotoxic chemicals as described in Supplementary Materials and Methods. The cells were incubated with anisomycin or 300 mmol/L NaCl for 30 min or 1 h, respectively. Cell extracts were prepared, and indicated proteins were detected by immunoblotting. β-Actin analysis serves as a loading control. *B*, parental HeLa cells were treated with anisomycin, and cell extracts were prepared at the indicated time to detect endogenous Cdc25A, Cdc25B, and Cdc25C. *C*, HeLa-W40 cells were treated with anisomycin or 50 μg/mL cycloheximide. Crude extracts were prepared at the indicated time, and the expression of Flag-Cdc25B was analyzed. *D*, HeLa cells constitutively expressing the Cdc25B^{DAA} mutant were treated with anisomycin or cycloheximide and the expression of Flag-Cdc25B proteins was determined by immunoblotting.

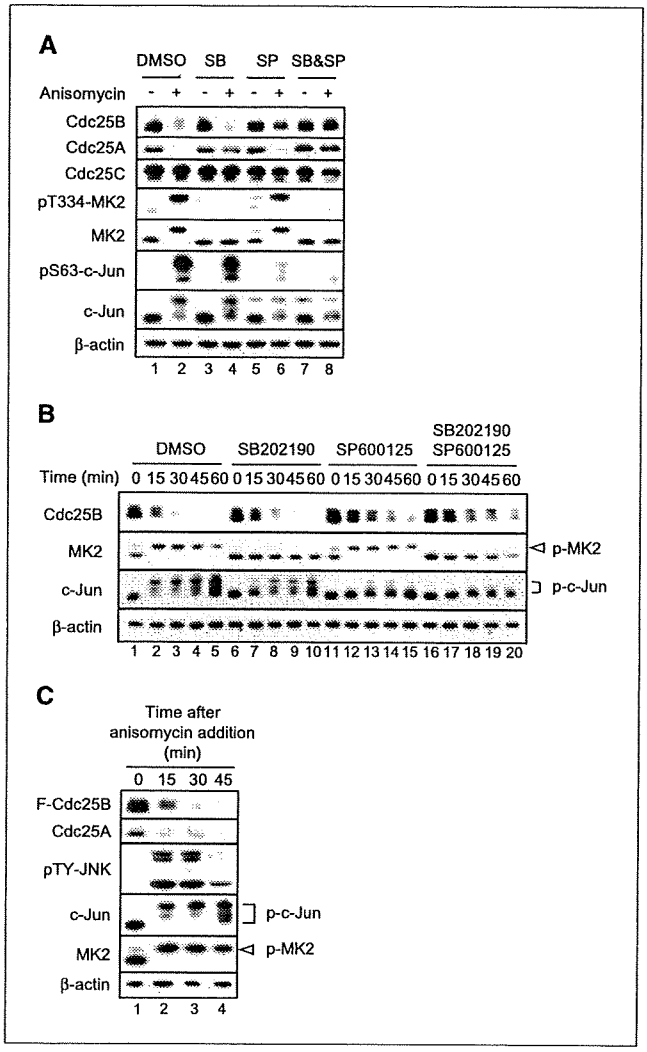

Figure 3. JNK inhibitor SP600125 attenuates the anisomycin-induced Cdc25B degradation. *A*, HeLa cells were treated with the indicated MAPK inhibitors for 1 h followed by anisomycin treatment. Cell extracts were prepared at 20 min after anisomycin addition. *SB*, SB202190; *SP*, SP600125. *B*, HeLa cells were treated with MAPK inhibitors, and the expression of proteins was determined at the indicated time. *C*, HeLa-W40 cells were treated with anisomycin, and the expression of protein was determined at the indicated time. Slower migrating bands of c-Jun and MK2 represent phosphorylated forms of the proteins.

Results of indirect immunofluorescence also supported that the instability of Cdc25B in anisomycin-treated cells was due to its proteasome-dependent degradation (Supplementary Fig. S3*D*).

The coexpression of either JNK1 or JNK2 with MKK7 triggered Cdc25B degradation (Fig. 4*A*). In addition, p38α was able to induce Cdc25B degradation. Furthermore, the expression of kinase-dead JNK1 and JNK2 stabilized Cdc25B (Fig. 4*B*), indicating dominant-negative effects. We further examined the contribution of MK2 to Cdc25B degradation. In this experiment, we used the D316N mutant of p38α, which is unable to activate MK2 (31). As shown in Fig. 4*C*, expression of $p38\alpha^{D316N}$ induced the degradation of Cdc25B. Taken together, these results suggest that JNK and p38 are integrally involved in Cdc25B degradation.

JNK phosphorylates Cdc25B. We found that bacterially expressed Cdc25B was phosphorylated by kinase-active JNK1 but not by its kinase-dead form, indication that JNK1 can directly phosphorylate Cdc25B (Supplementary Fig. S4*A*). Likewise, recombinant JNK1 could also phosphorylate Cdc25B (Supplementary Fig. S4*B*). To identify the phosphorylation site(s) on Cdc25B, GST fusion constructs of different fragments of Cdc25B were produced in *Escherichia coli* and used as substrates for kinase assays. As shown in Fig. 5*A*, JNK phosphorylation sites were present in the NH_2-terminal 175 amino acids. The same fragment was also phosphorylated by recombinant p38α (Supplementary Fig. S4*C*). Furthermore, JNK and Cdc25B were able to form complex, which supports the idea of Cdc25B being a JNK substrate [Supplementary Fig. S5*A*; the loss of the complex formation in wild-type (WT) JNK with MKK7 suggests that JNK may dislodge after phosphorylation event]. The importance of the NH_2-terminal region was also supported by the JNK-induced degradation of the construct containing green fluorescent protein fused to the NH_2-terminal 175 amino acid fragment of Cdc25B (Supplementary Fig. S5*B*).

Cdc25B/S101 is a candidate JNK phosphorylation site. To identify JNK phosphorylation site(s), we first mutated all six candidate serine residues to alanine in six potential JNK substrate SP sequences (and no TP) in N175-Cdc25B. The 6SA mutant was refractory to JNK- or p38α-induced degradation (Supplementary Fig. S6*A*). The coexpression of the individual SA mutant Cdc25B with JNK indicated the importance of S101, followed by S103 (Fig. 5*B*). The importance of S101 and S103 was further supported

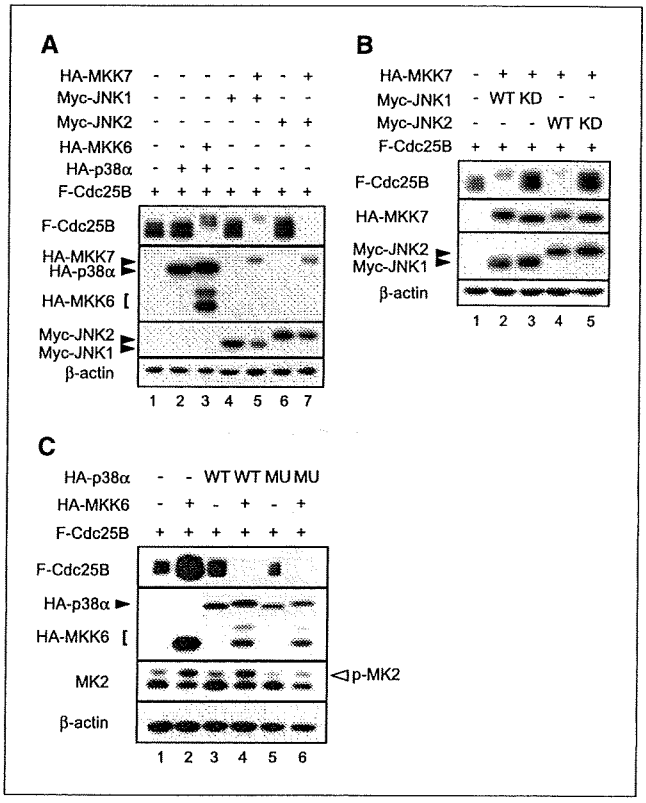

Figure 4. Involvement of JNK in the destabilization of Cdc25B. *A*, HeLa cells were transfected with Flag-Cdc25B in combination with MKK6 and p38α, or MKK7 and JNK1 or JNK2. The expression of the indicated proteins was determined by immunoblotting. *B*, expression of Flag-Cdc25B was determined after cotransfection with MKK7 and either the WT or kinase-dead (*KD*) form of JNK1 or JNK2. *C*, expression of Flag-Cdc25B was examined after cotransfection with MKK6 and WT or the D316N mutant (*MU*) of p38α. *Arrowhead*, phospho-MK2.

by the slower degradation rate of the Cdc25B protein with a double mutation (S101/103A) compared with the mutants with a single mutation (Fig. 5*C*, *lanes 4, 6*, and *8*). Essentially the same results were obtained when p38α was used as a kinase for the Cdc25B mutants (Supplementary Fig. S6*B*). Taken together, these data indicate that phosphorylation of Cdc25B at S101 and S103 by JNK and p38 is important for degradation.

HeLa cells expressing the Cdc25B S101A mutant ignore anisomycin-induced G_2 arrest. We next examined the effects of anisomycin on cell cycle progression, in particular during G_2-M phase, when Cdc25B peaks during the cell cycle. HeLa cells were synchronized at G_1-S and released into S phase. At 6 hours after release, the cells were treated with anisomycin followed by monitoring of M-phase entry by detection of phospho-S10-H3. Cdc25B and phospho-S10-H3 increased progressively in DMSO-treated cells (Fig. 6*A*), but no phospho-S10-H3 was detected in anisomycin-treated cells, indicating that anisomycin treatment inhibited mitotic entry. In such cells, Cdc25B disappeared completely by 30 minutes after addition of anisomycin (Fig. 6*A*, *lanes 7* and *8*). FACS analysis confirmed the induction of a G_2 delay by anisomycin treatment in synchronously or asynchronously growing HeLa cells (Supplementary Fig. S7*A*).

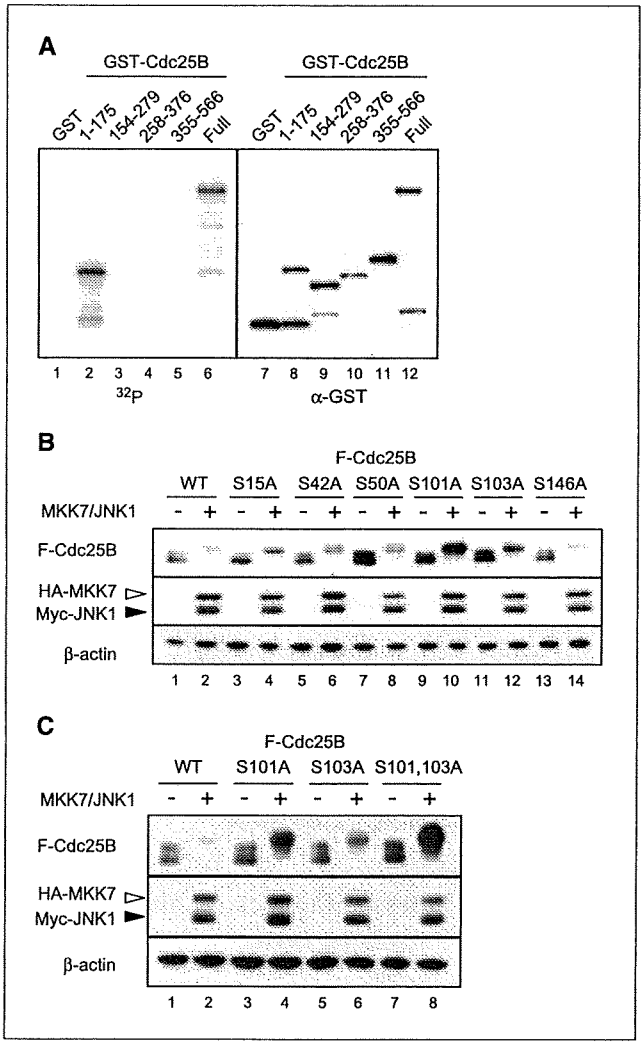

Figure 5. Phosphorylation of Cdc25B by JNK at possible phosphorylation sites. *A, left,* GST-Cdc25B fragments were incubated with a recombinant JNK1 in the presence of [γ-^{32}P]ATP followed by autoradiography; *right,* substrate GST-Cdc25B fragment as detected by anti-GST antibody. *B,* WT Cdc25B or mutants that contained SA mutations at candidate JNK phosphorylation sites were cotransfected into HeLa cells with or without MKK7 and JNK1, and expression of Cdc25B was determined by immunoblotting. *C,* the WT or SA mutant at S101, S103, or S101/103 was cotransfected into HeLa cells with or without MKK7 and JNK1, and the expression of Cdc25B was determined.

To delineate the significance of Cdc25B S101 phosphorylation in anisomycin-induced G_2 arrest, we added anisomycin to asynchronously growing HeLa cells that constitutively express the nonphosphorylatable Cdc25B S101A mutant (HeLa-101-1). The results shown in Fig. 6*B* indicate that the half-life of the S101A mutant Cdc25B was twice as long as that of the WT after anisomycin treatment (~35 minutes in S101A and ~15 minutes in WT), indicating that phosphorylation of S101 is essential for proper degradation. Treatment of HeLa-101-1 with either NaCl or UV also supported the idea that S101 is important for stress-induced Cdc25B degradation (Supplementary Fig. S8*A*).

We next investigated whether the S101A mutant would exhibit abrogation of anisomycin-induced G_2 arrest. We used cell lines expressing WT Cdc25B (W40) or S101A (101-1). The amount of Cdc25B protein in W40 cells and that of 101-1 is shown in Supplementary Fig. S7*B*. Asynchronously growing HeLa cells, W40 cells, and 101-1 cells were treated with 100 ng/mL anisomycin, and the number of cells entering M phase during a 3-hour treatment with anisomycin was determined by detecting phospho-S10-H3. As shown in Fig. 6*C*, HeLa-101-1 cells exhibited resistance to anisomycin-induced G_2 retardation. Thus, cells expressing S101A-mutated Cdc25B seem to be more resistant to anisomycin-induced degradation and to recover more rapidly than WT Cdc25B-expressing cells.

Collectively, HeLa cells expressing Cdc25B with a nonphosphorylatable mutation at the possible JNK target S101 residue were more refractory to anisomycin-induced cell cycle retardation.

Discussion

We report here for the first time that Cdc25B is targeted for degradation in cells that are challenged with anisomycin or NaCl and that the degradation of Cdc25B is mediated mainly by JNK. We uncovered this phenomenon by using HeLa cells that constitutively expressed recombinant Cdc25B. In our hands, commercially available antibodies did not properly recognize endogenous Cdc25B in crude extracts by immunoblotting. Immunoprecipitation followed by immunoblotting was necessary to detect endogenous Cdc25B.

Our experiments highlight the critical role of JNK in controlling Cdc25B stability. A level of DNA damage that is sufficient for activating Chk1/2 and Cdc25A degradation did not exert any effects on the stability of Cdc25B. Export of Cdc25B from the nucleus to the cytoplasm is thought to be a mechanism of checkpoint response (18). However, Cdc25B did not follow this expected pattern after DNA damage (Fig. 1*A*). We therefore suspect that Cdc25B is not a primary target of the DNA damage checkpoint, although we cannot exclude the possibility that its phosphatase activity is directly repressed by a Chk1-dependent mechanism (32).

We showed that M-phase entry is delayed in HeLa cells treated with anisomycin (Fig. 6). The G_2 retardation observed in this situation is caused in part by the degradation of Cdc25A and Cdc25B. Depletion of either Cdc25A or Cdc25B is insufficient for G_2-phase arrest, but the depletion of both Cdc25A and Cdc25B is necessary for a more robust G_2 arrest (4). Therefore, anisomycin-induced G_2

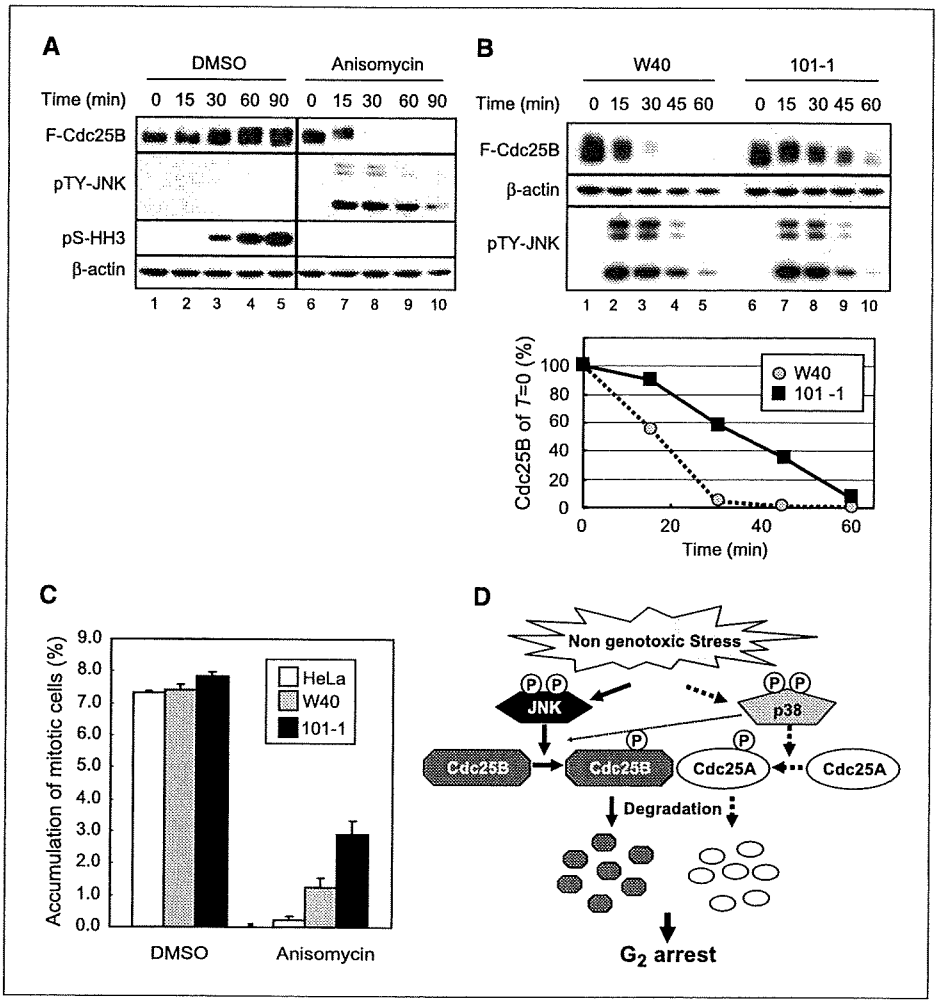

Figure 6. The Cdc25B mutant is refractory to anisomycin-induced G_2 arrest. *A*, HeLa cells synchronized at G_1-S were released into the cell cycle for 6 h, followed by the addition of anisomycin. At the indicated times, the expression of proteins was determined. *B*, HeLa-W40 or HeLa-101-1 cells were treated with anisomycin, and the expression of the proteins was determined at the indicated time points after treatment. *Bottom*, quantitative results. Typical results of three independent experiments are shown. *C*, asynchronously growing HeLa, HeLa-W40, or HeLa-101-1 cells were treated with 100 ng/mL anisomycin and 100 ng/mL nocodazole for 3 h. Cells were collected, and the cells in M phase were determined by detecting phospho-histone H3-Ser^{10} by FACS. *Columns*, mean of three independent experiments; *bars*, SD. The percentage of mitotic cells in asynchronous cells was as follows: HeLa, 2.76 ± 0.27; W40, 3.57 ± 0.13; 101-1, 3.61 ± 0.14. *D*, a model of the induction of Cdc25A and Cdc25B degradation after nongenotoxic stress followed by G_2 arrest.

retardation can be explained at least in part by the simultaneous degradation of Cdc25A and Cdc25B (Fig. 2). Our results strongly suggest the presence of a nongenotoxic stress–dependent cell cycle checkpoint wherein Cdc25 phosphatases are degraded to down-regulate CDK activity. This checkpoint is mediated by stress-activated MAPKs, including p38 and JNK, as depicted in Fig. 6*D*. The proteasome inhibitor MG132 attenuated anisomycin-induced Cdc25B degradation, which strongly suggests that Cdc25B is degraded by the ubiquitin-proteasome pathway. Cdc25B is degraded in the steady state by the $SCF^{\beta\text{-}TrCP}$–mediated ubiquitinylation mechanism. It is unlikely that phosphorylation of S101 stimulated binding of $SCF^{\beta\text{-}TrCP}$ to the constitutive binding site, which is located more than 100 amino acids downstream of S101. It is necessary to identify the responsible ubiquitinylation system to understand JNK-mediated Cdc25B degradation more precisely.

Several reports have indicated a correlation between the malignancy of tumors and the overexpression of Cdc25A and Cdc25B (33, 34). Cdc25A and Cdc25B are oncogenic (35), and Cdc25A is a main target of the DNA damage checkpoint (1, 2, 34). Assuming that Cdc25B is a target of a nongenotoxic stress checkpoint, overexpression of Cdc25B may allow cells to become less sensitive to intrinsically harmful cell stresses that do not directly compromise genome integrity. Ignoring the detrimental stress signal, such as NaCl-induced distortion of the cytoskeleton by hyperosmolarity or anisomycin-induced inhibition of protein synthesis, may disrupt the proper regulation of chromosome segregation and cytokinesis during mitosis, which are well-known causative events of genome instability (36).

In conclusion, we have shown that Cdc25B is targeted for JNK-mediated degradation by cellular stress. The stress-induced checkpoint is initiated by the activation of JNK and p38, which phosphorylates Ser^{101} of Cdc25B. This results in the rapid degradation of Cdc25B and cell cycle arrest.

Disclosure of Potential Conflicts of Interest

No potential conflicts of interest were disclosed.

Acknowledgments

Received 3/6/09; revised 4/22/09; accepted 6/3/09; published OnlineFirst 7/28/09.

Grant support: Long-range Research Initiative of the Japan Chemical Industry Association; Ministry of Health, Labor, and Welfare of Japan; Japan Society for the Promotion of Science; and Yamagiwa-Yoshida Fellowship from the International Union Against Cancer, Switzerland.

The costs of publication of this article were defrayed in part by the payment of page charges. This article must therefore be hereby marked *advertisement* in accordance with 18 U.S.C. Section 1734 solely to indicate this fact.

We thank Dr. H. Shima for the p38α plasmid and Dr. M. Ogata for information on the *sevenmaker* mutation of MAPKs.

References

1. Bartek J, Lukas J. Mammalian G_1- and S-phase checkpoints in response to DNA damage. Curr Opin Cell Biol 2001;13:738–47.
2. Busino L, Chiesa M, Draetta GF, Donzelli M. Cdc25A phosphatase: combinatorial phosphorylation ubiquitylation and proteolysis. Oncogene 2004;23:2050–6.
3. Mailand N, Podtelejnikov AV, Groth A, Mann M, Bartek J, Lukas J. Regulation of G_2/M events by Cdc25A through phosphorylation-dependent modulation of its stability. EMBO J 2002;21:5911–20.
4. Lindqvist A, Källström H, Lundgren A, Barsoum E, Rosenthal CK. Cdc25B cooperates with Cdc25A to induce mitosis but has a unique role in activating cyclin B1-Cdk1 at the centrosome. J Cell Biol 2005;171:35–45.
5. Bartek J, Lukas J. Chk1 and Chk2 kinases in checkpoint control and cancer. Cancer Cell 2003;3:421–9.
6. Jin J, Shirogane T, Xu L, et al. $SCF^{\beta\text{-}TRCP}$ links Chk1 signaling to degradation of the Cdc25A protein phosphatase. Genes Dev 2003;17:3062–74.
7. Chen MS, Hurov J, White LS, Woodford-Thomas T, Piwnica-Worms H. Absence of apparent phenotype in mice lacking Cdc25C protein phosphatase. Mol Cell Biol 2001;21:3853–61.
8. Ferguson AM, White LS, Donovan PJ, Piwnica-Worms H. Normal cell cycle and checkpoint responses in mice and cells lacking Cdc25B and Cdc25C protein phosphatases. Mol Cell Biol 2005;25:2853–60.
9. Lincoln AJ, Wickramasinghe D, Stein P, et al. Cdc25b phosphatase is required for resumption of meiosis during oocyte maturation. Nat Genet 2002;30:446–9.
10. Dutertre S, Cazales M, Quaranta M, et al. Phosphorylation of CDC25B by Aurora-A at the centrosome contributes to the G_2-M transition. J Cell Sci 2004;117:2523–31.
11. Kramer A, Mailand N, Lukas C, et al. Centrosome-associated Chk1 prevents premature activation of cyclin-B-Cdk1 kinase. Nat Cell Biol 2004;6:884–91.
12. Schmitt E, Boutros R, Froment C, Monsarrat B, Ducommun B, Dozier C. CHK1 phosphorylates CDC25B during the cell cycle in the absence of DNA damage. J Cell Sci 2006;119:4269–75.
13. Uchida S, Kuma A, Ohtsubo M, et al. Binding of 14-3-3β but not 14-3-3σ controls the cytoplasmic localization of CDC25B: binding site preferences of 14-3-3 subtypes and the subcellular localization of CDC25B. J Cell Sci 2004;117:3011–20.
14. Boutros R, Dozier C, Ducommun B. The when and where of CDC25 phosphatases. Curr Opin Cell Biol 2006;18:185–91.
15. Forrest A, Gabrielli B. Cdc25B activity is regulated by 14-3-3. Oncogene 2001;20:4393–401.
16. Davezac N, Baldin V, Gabrielli B, et al. Regulation of CDC25B phosphatases subcellular localization. Oncogene 2000;19:2179–85.
17. Johnson GL, Lapadat R. Mitogen-activated protein kinase pathways mediated by ERK JNK and p38 protein kinases. Science 2002;298:1911–2.
18. Manke IA, Nguyen A, Lim D, Stewart MQ, Elia AE, Yaffe MB. MAPKAP kinase-2 is a cell cycle checkpoint kinase that regulates the G_2/M transition and S phase progression in response to UV irradiation. Mol Cell 2005;17:37–48.
19. Bulavin DV, Amundson SA, Fornace AJ. p38 and Chk1 kinases: different conductors for the G_2/M checkpoint symphony. Curr Opin Genet Dev 2002;12:92–7.
20. Goloudina A, Yamaguchi H, Chervyakova DB, Appella E, Fornace AJ, Jr., Bulavin DV. Regulation of human Cdc25A stability by serine 75 phosphorylation is not sufficient to activate an S phase checkpoint. Cell Cycle 2003;2:473–8.
21. Goss VL, Cross JV, Ma K, Qian Y, Mola PW, Templeton DJ. SAPK/JNK regulates cdc2/cyclin B kinase through phosphorylation and inhibition of cdc25C. Cell Signal 2003;15:709–18.
22. Lindqvist A, Källström H, Karlsson-Rosenthal C. Characterisation of Cdc25B localisation and nuclear export during the cell cycle and in response to stress. J Cell Sci 2004;117:4979–90.
23. Uchida S, Ohtsubo M, Shimura M, et al. Nuclear export signal in CDC25B. Biochem Biophys Res Commun 2004;316:226–32.
24. Uchida S, Kubo A, Kizu R, et al. Amino acids C-terminal to the 14-3-3 binding motif in CDC25B affect the efficiency of 14-3-3 binding. J Biochem (Tokyo) 2006;139:761–9.
25. Bulavin DV, Higashimoto Y, Popoff IJ, et al. Initiation of a G_2/M checkpoint after ultraviolet radiation requires p38 kinase. Nature 2001;411:102–7.
26. Lemaire M, Froment C, Boutros R, et al. CDC25B phosphorylation by p38 and MK-2. Cell Cycle 2006;5:1649–53.
27. Rogakou EP, Pilch DR, Orr AH, Ivanova VS, Bonner WM. DNA double-stranded breaks induce histone H2AX phosphorylation on serine 139. J Biol Chem 1998;273:5858–68.
28. Cano E, Hazzalin CA, Mahadevan LC. Anisomycin-activated protein kinases p45 and p55 but not mitogen-activated protein kinases ERK-1 and -2 are implicated in the induction of c-fos and c-jun. Mol Cell Biol 1994;14:7352–62.
29. Iordanov MS, Pribnow D, Magun JL, et al. Ribotoxic stress response: activation of the stress-activated protein kinase JNK1 by inhibitors of the peptidyl transferase reaction and by sequence-specific RNA damage to the α-sarcin/ricin loop in the 28S rRNA. Mol Cell Biol 1997;17:3373–81.
30. Kanemori Y, Uto K, Sagata N. β-TrCP recognizes a previously undescribed nonphosphorylated destruction motif in Cdc25A and Cdc25B phosphatases. Proc Natl Acad Sci U S A 2005;102:6279–84.
31. Hutter D, Chen O, Barnes J, Liu Y. Catalytic activation of mitogen-activated protein (MAP) kinase phosphatase-1 by binding to p38 MAP kinase: critical role of the p38 C-terminal domain in its negative regulation. Biochem J 2000;352:155–63.
32. Uto K, Inoue D, Shimuta K, Nakajo N, Sagata N. Chk1 but not Chk2 inhibits Cdc25 phosphatases by a novel common mechanism. EMBO J 2004;23:3386–96.
33. Kristjánsdóttir K, Rudolph J. Cdc25 phosphatases and cancer. Chem Biol 2004;11:1043–51.
34. Boutros R, Lobjois J, Ducommun B. CDC25 phosphatases in cancer cells: key players? Good targets? Nat Rev Cancer 2007;7:495–507.
35. Galaktionov K, Lee AK, Eckstein J, et al. CDC25 phosphatases as potential human oncogenes. Science 1995;269:1575–7.
36. Kops GJ, Weaver BA, Cleveland DW. On the road to cancer: aneuploidy and the mitotic checkpoint. Nat Rev Cancer 2005;5:773–85.

Molecular Biology of the Cell
Vol. 20, 2186–2195, April 15, 2009

The Extracellular Signal-regulated Kinase–Mitogen-activated Protein Kinase Pathway Phosphorylates and Targets Cdc25A for SCF$^{\beta\text{-TrCP}}$-dependent Degradation for Cell Cycle Arrest

Michitaka Isoda,* Yoshinori Kanemori,* Nobushige Nakajo,* Sanae Uchida[†‡] Katsumi Yamashita,[†] Hiroyuki Ueno,* and Noriyuki Sagata*[§]

*Department of Biology, Graduate School of Sciences, Kyushu University, Hakozaki 6-10-1, Fukuoka 812-8581, Japan; [†]Division of Life Science, Graduate School of Natural Science and Technology; [‡]Venture Business Laboratory, Center for Innovation, Kanazawa University, Kanazawa 920-1192, Ishikawa, Japan; and [§]CREST, Japan Science and Technology Agency, Nihonbashi, Tokyo 103-0027, Japan

Submitted January 6, 2009; Revised February 18, 2009; Accepted February 18, 2009
Monitoring Editor: Daniel J. Lew

The extracellular signal-regulated kinase (ERK) pathway is generally mitogenic, but, upon strong activation, it causes cell cycle arrest by a not-yet fully understood mechanism. In response to genotoxic stress, Chk1 hyperphosphorylates Cdc25A, a positive cell cycle regulator, and targets it for Skp1/Cullin1/F-box protein (SCF)$^{\beta\text{-TrCP}}$ ubiquitin ligase-dependent degradation, thereby leading to cell cycle arrest. Here, we show that strong ERK activation can also phosphorylate and target Cdc25A for SCF$^{\beta\text{-TrCP}}$-dependent degradation. When strongly activated in *Xenopus* eggs, the ERK pathway induces prominent phosphorylation and SCF$^{\beta\text{-TrCP}}$-dependent degradation of Cdc25A. p90rsk, the kinase downstream of ERK, directly phosphorylates Cdc25A on multiple sites, which, interestingly, overlap with Chk1 phosphorylation sites. Furthermore, ERK itself phosphorylates Cdc25A on multiple sites, a major site of which apparently is phosphorylated by cyclin-dependent kinase (Cdk) in Chk1-induced degradation. p90rsk phosphorylation and ERK phosphorylation contribute, roughly equally and additively, to the degradation of Cdc25A, and such Cdc25A degradation occurs during oocyte maturation in which the endogenous ERK pathway is fully activated. Finally, and importantly, ERK-induced Cdc25A degradation can elicit cell cycle arrest in early embryos. These results suggest that strong ERK activation can target Cdc25A for degradation in a manner similar to, but independent of, Chk1 for cell cycle arrest.

INTRODUCTION

The Cdc25A phosphatase, a key cell cycle regulator in vertebrates, dephosphorylates and activates cyclin-dependent kinases (Cdks), thereby promoting cell cycle progression (Donzelli and Draetta, 2003). On genotoxic stress, however, the checkpoint kinases Chk1 and Chk2 hyperphosphorylate Cdc25A and target it for rapid degradation, thereby inducing cell cycle arrest for DNA repair (Bartek and Lukas, 2003). In human cells, Chk1 phosphorylation promotes the binding of β-transducing repeat-containing protein (β-TrCP), the F-box protein of the Skp1/Cullin1/F-box protein (SCF)$^{\beta\text{-TrCP}}$ ubiquitin ligase (Frescas and Pagano, 2008), to the doubly phosphorylated DSG motif (DpSGX$_{2-4}$pS) of Cdc25A and thereby targets the phosphatase for degradation (Busino *et al.*, 2003; Jin *et al.*, 2003). In *Xenopus* eggs and embryos, activated Chk1 also phosphorylates and targets *Xenopus* Cdc25A for SCF$^{\beta\text{-TrCP}}$-dependent degradation, but, in this case, by promoting the binding of β-TrCP to the nonphosphorylated DDG motif (DDGX$_2$D) (which also exists and functions in human Cdc25A) (Shimuta *et al.*, 2002; Kanemori *et al.*, 2005). In both human and *Xenopus* Cdc25A proteins, however, Chk1 phosphorylates multiple conserved Arg-X-X-Ser motifs in the N-terminal regulatory domain (Busino *et al.*, 2003; Uto *et al.*, 2004). Although phosphorylation of a conserved Ser-Pro motif is also required for the Chk1-induced degradation of human Cdc25A, the responsible kinase is not known (Busino *et al.*, 2003).

Mitogen-activated protein kinase (MAPK) pathways regulate diverse cellular processes ranging from proliferation and differentiation to apoptosis. In vertebrates, there are three major MAPK signaling pathways: extracellular signal-regulated kinase (ERK), Jun NH$_2$-terminal kinase (JNK), and p38 MAPK pathways (Raman *et al.*, 2007). The ERK pathway is mainly activated by mitogenic stimuli, such as growth factors and phorbol esters (Meloche and Pouyssegur, 2007). In contrast, the JNK pathway is activated by radiation and other environmental stresses, whereas the p38 pathway is activated by numerous stresses, such as UV irradiation, cytokines, and osmotic shock (Raman *et al.*, 2007). Interestingly, the p38 pathway is involved in the degradation of Cdc25A that occurs in response to UV irradiation and interleukin withdrawal in certain mammalian cells (Khaled *et al.*,

This article was published online ahead of print in *MBC in Press* (http://www.molbiolcell.org/cgi/doi/10.1091/mbc.E09-01-0008) on February 25, 2009.

Address correspondence to: Noriyuki Sagata (nsagascb@mbox.nc.kyushu-u.ac.jp or nsagascb@kyushu-u.org).

Abbreviations used: ERK, extracellular signal-regulated kinase; MAPK, mitogen-activated protein kinase; Mkp3, mitogen-activated protein kinase phosphatase 3; SCF, Skp1/Cullin1/F-box protein; Xe, *Xenopus*.

2005; Reinhardt *et al.*, 2007). This Cdc25A degradation is important for cell cycle arrest that follows, but its mechanism is poorly understood (Reinhardt *et al.*, 2007).

Whereas weak or sustained activation of the ERK pathway is generally mitogenic, its strong activation by oncogenic Ras or activated Raf causes differentiation in certain cell types and cell cycle arrest (and senescence) in many cell types (Ebisuya *et al.*, 2005; Meloche and Pouyssegur, 2007). This cell cycle arrest has been suggested to be elicited by the ERK-mediated up-regulation of negative cell cycle regulators, such as p53 and Cdk inhibitors (such as $p21^{Cip1}$ and $p16^{Ink4a}$) (Pumiglia and Decker, 1997; Serrano *et al.*, 1997; Zhu *et al.*, 1998; Meloche and Pouyssegur, 2007). Although hitherto not recognized, however, such cell cycle arrest might also be contributed to by an ERK-dependent down-regulation of some positive cell cycle regulator(s).

In this study, we have investigated whether strong ERK activation can induce down-regulation (or degradation) of the positive cell cycle regulator Cdc25A. We show that the ERK pathway, when strongly activated in *Xenopus* eggs, phosphorylates and targets Cdc25A for degradation. This degradation involves the $SCF^{\beta\text{-}TrCP}$ ubiquitin ligase and requires phosphorylations by both ERK and its downstream kinase p90rsk. Furthermore, strong ERK activation can cause cell cycle arrest in early embryos by targeting Cdc25A for degradation. These results, together with other results, suggest that, unexpectedly, the ERK pathway can target Cdc25A for degradation in a manner very similar to Chk1 and that Cdc25A degradation contributes to cell cycle arrest caused by strong ERK activation.

MATERIALS AND METHODS

Oocytes, Eggs, and Embryos

Oocytes, unfertilized eggs, and embryos were prepared, microinjected, and cultured as described previously (Kanemori *et al.*, 2005; Inoue *et al.*, 2007). Oocyte maturation and artificial egg activation were induced by progesterone (5 mg/ml) and the calcium ionophore A23187 (1 mg/ml), respectively, as described previously (Kanemori *et al.*, 2005; Inoue *et al.*, 2007). Artificially activated eggs are a very good system (for their single-cell nature) to express exogenous proteins (by mRNA injection) and to analyze regulation of cell cycle regulators, such as Cdc25A and Wee1 (Kanemori *et al.*, 2005; Okamoto and Sagata, 2007). We usually used the eggs after 40 min of artificial activation.

cDNAs and In Vitro Transcription

cDNAs encoding *Xenopus* Cdc25A, a constitutively active form of *Xenopus* p90rsk, and a dominant-negative mutant of *Xenopus* β-TrCP were described previously (Shimuta *et al.*, 2002; Kanemori *et al.*, 2005; Inoue *et al.*, 2007). cDNAs encoding mouse mitogen-activated protein kinase kinase (MKK) 1 or MAP kinase-ERK kinase (MEK) 1 (accession number NM 008927), human MKK6 (NM 002758), *Xenopus* MKK7 (NM 001087648), *Xenopus* JNKa (AB073999), human $p21^{Cip1}$ (NM 000389), and human MKP3 (NM 001946) were isolated by polymerase chain reaction (PCR) from appropriate cDNA libraries. A constitutively active form of MEK1 was made by deleting the region encompassing amino acids 32–51 and by mutating two serine residues (Ser-218→Asp, Ser-222→Glu) (Mansour *et al.*, 1994). A constitutively active form of MKK6 was made by mutating two residues (Ser-207→Asp, Thr-211→Asp) (Alonso *et al.*, 2000), whereas that of MKK7 by mutating three residues (Ser-268→Asp, Thr-272→Glu, Ser-274→Asp) (Yamanaka *et al.*, 2002). All the cDNA constructs were subcloned into either the N-terminally Myc-tagged or glutathione *S*-transferase (GST)-tagged pT7-G (UKII-) transcription vectors (Uto *et al.*, 2004; Kanemori *et al.*, 2005). In vitro mutagenesis and transcription of the cDNAs were performed as described previously (Shimuta *et al.*, 2002).

In Vitro Translation

In vitro translation of Xe-Cdc25A mRNA was performed using wheat germ extracts (L4380; Promega, Madison, WI) as described previously (Inoue *et al.*, 2007).

GST Fusion Proteins

cDNAs encoding *Xenopus* Cdc25A peptides (S36, residues 16-56; S85, 58-102; S120, 91-136; S129, 104-154; S137, 120-168; S190, 166-215; S198, 175-213; and S295, 265-316) and their Ser→Ala mutant peptides were subcloned into the pGEX-3X plasmid vector, and the GST-fused peptides were bacterially expressed and purified by standard methods.

Morpholino Oligonucleotides (Oligos)

Antisense morphlino oligos against *Xenopus* Erp1 mRNA were prepared and injected into one-cell embryos as described previously (Inoue *et al.*, 2007).

In Vitro Kinase Assays

For in vitro p90rsk and ERK kinase assays, GST-fused Xe-Cdc25A peptides were incubated with [γ-^{32}P]ATP and either p90rsk2 protein (14–480; Millipore, Billerica, MA) or ERK2 protein (P6080; New England Biolabs, Ipswich, MA) and analyzed essentially as described previously (Inoue *et al.*, 2007). In vitro translated Xe-Cdc25A protein was incubated with ERK2 protein in the absence of [γ-^{32}P]ATP as described previously (Inoue *et al.*, 2007).

Antibodies and Immunoblotting

Anti-*Xenopus* Cdc25A phospho-Ser-85 antibody was raised in rabbits against peptides (LDpSPIKMDLRC) and affinity-purified by standard methods. Routinely, proteins equivalent to one oocyte or egg were analyzed by immunoblotting using anti-*Xenopus* Cdc25A antibody (Shimuta *et al.*, 2002), anti-Myc antibody (A-14; Santa Cruz Biotechnology, Santa Cruz, CA), anti-GST antibody (Z-5; Santa Cruz Biotechnology), anti-phospho-p44/42 MAPK antibody (9106; Cell Signaling Technology, Danvers, MA), anti-phospho-JNK antibody (9251; Cell Signaling Technology), anti-phospho-p38 antibody (9211; Cell Signaling Technology), anti-Cdk1 phospho-Thr-14/Tyr-15 antibody (44–686G; BioSource International, Camarillo, CA), anti-*Xenopus* Erp1 antibody (Inoue *et al.*, 2007), or anti-*Xenopus* Cdc25A phospho-Ser-85 antibody, essentially as described previously (Uto *et al.*, 2004). In some experiments, oocyte or egg extracts before immunoblotting were treated with λ phosphatase as described previously (Inoue *et al.*, 2007).

RESULTS

Activation of ERK Induces Degradation of Xe-Cdc25A in Xenopus Eggs

First, we examined whether strong activation of ERK, p38, or JNK MAPKs could induce degradation of Cdc25A. For this, we ectopically expressed, by mRNA injection, their immediate upstream activators (MKKs) in artificially activated *Xenopus* eggs, and then monitored activating phosphorylation of endogenous MAPKs and the levels of endogenous Cdc25A (Xe-Cdc25A) by immunoblotting. Activated eggs (which mimic fertilized eggs) are a very good in vivo system to reproducibly analyze regulatory mechanisms of cell cycle regulators, such as Cdc25A and Wee1 (Kanemori *et al.*, 2005; Okamoto and Sagata, 2007; see *Materials and Methods*). Ectopic expression of a constitutively active (CA) form of MKK6, an activator of p38, efficiently induced activating phosphorylation of endogenous p38 but only very weakly induced the mobility shift and degradation of Xe-Cdc25A (Figure 1A, MKK6-CA) (see *Discussion*). Expression of a CA form of MKK7 (a JNK activator) (together with JNK; Lei *et al.*, 2002) did not induce any appreciable mobility shift or degradation of Xe-Cdc25A (Figure 1A, MKK7-CA + JNK). In contrast to these, expression of a CA form of MEK1 (or MKK1), an activator of ERK, strongly induced both mobility upshifts (due to phosphorylation; Figure 1B) and degradation of Xe-Cdc25A (Figure 1A, MEK-CA). In this experiment, however, MEK-CA expression induced activating phosphorylation of not only ERK but also JNK (Figure 1A, MEK-CA). However, JNK activation after MEK-CA expression was far much weaker than that after MKK7-CA expression, which itself could not induce any mobility shift or degradation of Xe-Cdc25A (Figure 1A, MKK7-CA + JNK). Thus, these results suggest that strong activation of the MEK/ERK pathway can specifically induce prominent phosphorylation and degradation of endogenous Xe-Cdc25A in *Xenopus* eggs.

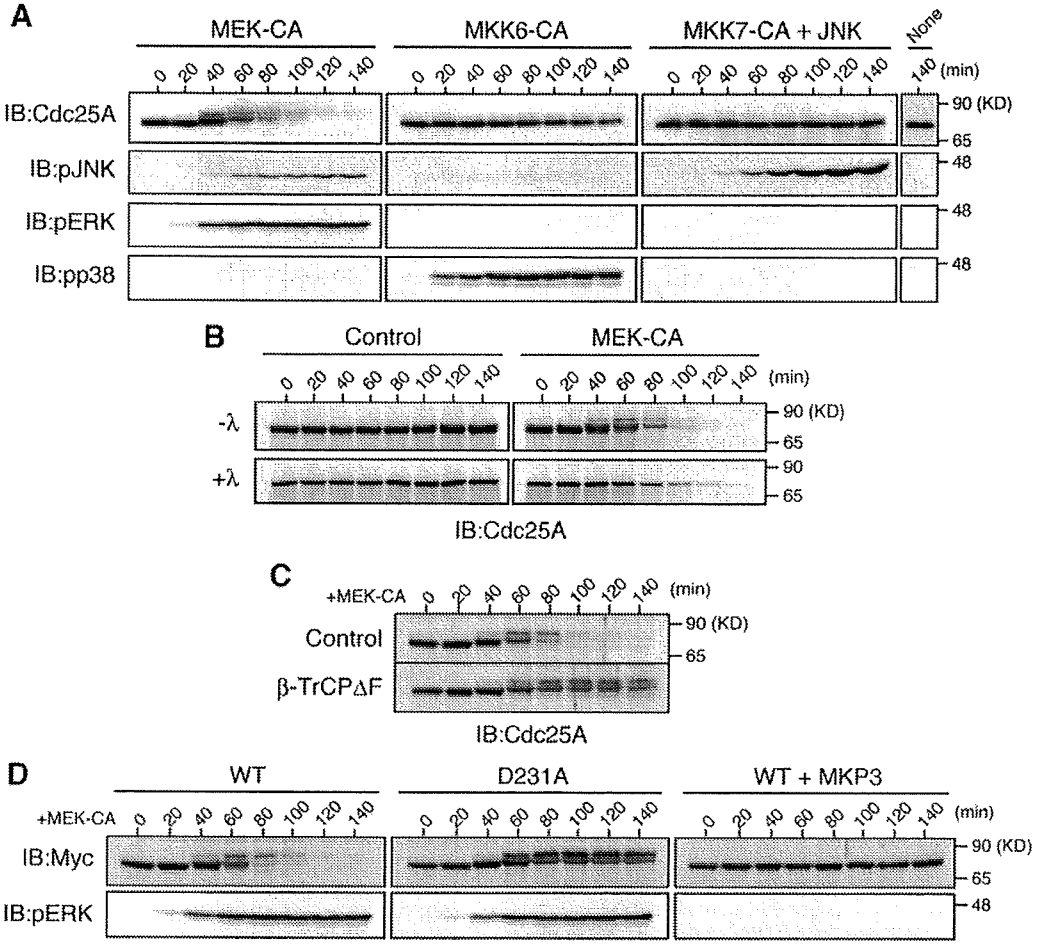

Figure 1. Induction of $SCF^{\beta\text{-}TrCP}$-dependent degradation of Xe-Cdc25A by the ERK pathway. (A) Artificially activated eggs (or eggs after 40 min of calcium ionophore treatment) were injected or not with 9 ng of JNK mRNA, reinjected 2.5 h later (time 0) with 9 ng of either MEK-CA, MKK6-CA, or MKK7-CA mRNAs, and analyzed at 20-min intervals by immunoblotting (IB) with anti-Xe-Cdc25A, anti-phospho-JNK, anti-phospho-ERK, and anti-phospho-p38 antibodies. (B) Activated eggs were injected with 9 ng of GST mRNA (Control) or MEK-CA mRNA. Egg extracts were then treated (+λ) or not (−λ) with λ phosphatase and analyzed for Xe-Cdc25A by immunoblotting. (C) Activated eggs were injected with 18 ng of GST mRNA (Control) or dominant-negative β-TrCPΔF mRNA, reinjected 2.5 h later with 9 ng of MEK-CA mRNA, and then analyzed for Xe-Cdc25A by immunoblotting. (D) Activated eggs were injected or not with 9 ng of MKP3 mRNA, reinjected 40 min later with 2 ng of mRNA encoding Myc-tagged WT or D231A Xe-Cdc25A, further injected 2.5 h later with 9 ng of MEK-CA mRNA, and then analyzed for Myc-Xe-Cdc25A constructs and phospho-ERK by immunoblotting. Five, three, four, and four independent experiments were performed for A, B, C, and D, respectively, and, for each, a typical result is shown.

Involvement of $SCF^{\beta-TrCP}$ in the ERK-induced Degradation of Xe-Cdc25A

Interestingly, the kinetics of phosphorylation and degradation of Xe-Cdc25A after MEK-CA expression (or ERK activation) in activated eggs is very similar to that after Chk1 activation in the same egg system (Shimuta *et al.*, 2002; Kanemori *et al.*, 2005). However, Chk1 itself was apparently not involved in the MEK-CA–induced phosphorylation or degradation of Xe-Cdc25A, because Chk1 was not activated at all in MEK-CA–expressing eggs (data not shown), just as in normal eggs (Shimuta *et al.*, 2002). Nevertheless, given the similar phosphorylation and degradation of Xe-Cdc25A, MEK-CA-induced Xe-Cdc25A degradation might be mediated by the $SCF^{\beta\text{-}TrCP}$ ubiquitin ligase, which is involved in Chk1-induced Xe-Cdc25A degradation (Kanemori *et al.*, 2005). To test this possibility, we overexpressed a dominant-negative mutant of β-TrCP (β-TrCPΔF) in activated eggs (Kanemori *et al.*, 2005). This treatment prevented the degradation (but not phosphorylation) of endogenous Xe-Cdc25A after MEK-CA expression (Figure 1C). Furthermore, when ectopically expressed in eggs, a Myc-tagged, Asp-231→Ala mutant of Xe-Cdc25A (D231A), i.e., the DDG motif mutant that cannot bind β-TrCP upon Chk1 activation (Kanemori *et al.*, 2005), was extremely stable even after expression of MEK-CA (Figure 1D). In these experiments, even Xe-Cdc25A WT was very stable (and apparently not phosphorylated) if MKP3, an ERK (but not MEK)-inactivating phosphatase (Muda *et al.*, 1996), was coexpressed with MEK-CA (Figure 1D). These results, together with the above-mentioned results (Figure 1A), strongly suggest that the MEK/ERK pathway, only downstream of MEK, phosphorylates Xe-Cdc25A and targets it for $SCF^{\beta\text{-}TrCP}$-dependent degradation.

Phosphorylation of Xe-Cdc25A by p90rsk and Its Contribution to ERK-induced Xe-Cdc25A Degradation

We attempted to identify the phosphorylation site(s) required for Xe-Cdc25A degradation after ERK activation.

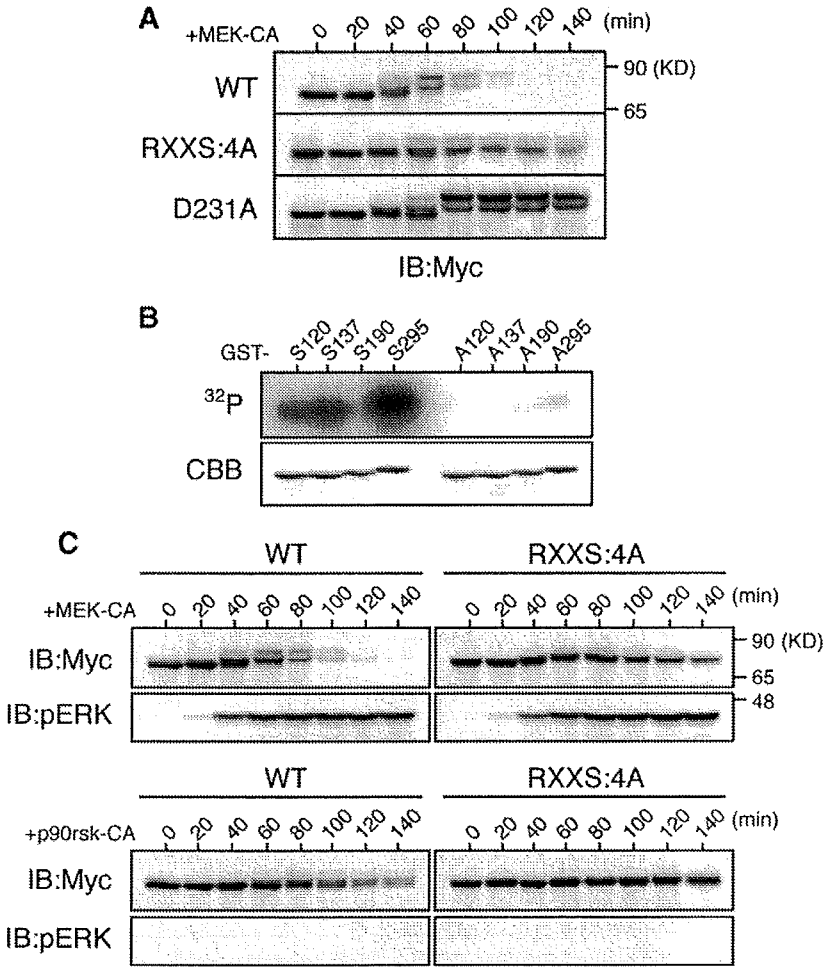

Figure 2. p90rsk phosphorylation, and its requirement for the ERK pathway-induced degradation, of Xe-Cdc25A. (A) Activated eggs were injected with 2 ng of mRNA encoding the indicated Myc-Xe-Cdc25A constructs, reinjected 2.5 h later with 9 ng of MEK-CA mRNA, and then analyzed for Myc-Xe-Cdc25A constructs by immunoblotting. (B) GST-fused Xe-Cdc25A peptides (GST-S120, GST-A120, etc., each named after the relevant Ser or substituted Ala residue numbers) were incubated with [γ-^{32}P]ATP and p90rsk protein, subjected to SDS-polyacrylamide gel electrophoresis, stained with Coomassie Brilliant Blue (CBB), and then autoradiographed (^{32}P). (C) Activated eggs were injected with 2 ng of mRNA encoding the indicated Myc-Xe-Cdc25A constructs, reinjected 2.5 h later with either 9 ng of MEK-CA mRNA or 36 ng of p90rsk-CA mRNA, and analyzed for Myc-Xe-Cdc25A constructs and phospho-ERK by immunoblotting. Four, three, and four independent experiments were performed for A, B, and C, respectively, and, for each, a typical result is shown.

Previously, we showed that phosphorylation by Chk1 of four Ser residues (S120, S137, S190, and S295) in the Arg-X-X-Ser (RXXS) motifs is required for the Chk1-induced degradation of Xe-Cdc25A (Uto *et al.*, 2004). We therefore asked whether these Ser residues would be required for ERK-induced Xe-Cdc25A degradation. When expressed in activated eggs, a Xe-Cdc25A mutant in which all of the four Ser residues were mutated to Ala (RXXS:4A) was significantly more stable than the wild type (WT), although not as stable as the completely stable D231A mutant, after MEK-CA expression (Figure 2A). Furthermore, the RXXS:4A mutant was somewhat less phosphorylated than the WT, as evidenced by its smaller size shifts, after MEK-CA expression (Figure 2A). Thus, intriguingly, the ERK pathway seems to phosphorylate at least some Chk1 phosphorylation sites for Xe-Cdc25A degradation.

We noted that, like Chk1, p90rsk, the kinase downstream of ERK (Sturgill *et al.*, 1988), belongs to the Ca^{2+}/calmodulin-regulated kinase subfamily of protein kinases and can phosphorylate RXXS motifs in its substrates (Frodin and Gammeltoft, 1999; Inoue *et al.*, 2007). We therefore first tested whether p90rsk could phosphorylate any of the four Chk1 phosphorylation sites in Xe-Cdc25A. When analyzed by in vitro kinase assays using [γ-^{32}P]ATP and GST-fused Xe-Cdc25A peptides (with or without Ala substitution), three (S120, S137, and S295) of the four Ser residues were significantly phosphorylated by p90rsk (Figure 2B). We then addressed whether ectopic expression of a constitutively active form of p90rsk (p90rsk-CA) can induce degradation of Xe-Cdc25A (WT or RXXS:4A) in activated eggs. Xe-Cdc25A WT was degraded after p90rsk-CA expression, albeit significantly less efficiently than after MEK-CA expression; notably, however, the RXXS:4A mutant was completely stable even after p90rsk-CA expression, although it was somewhat degraded after MEK-CA expression (Figure 2C). Together, these results suggest that p90rsk can phosphorylate Xe-Cdc25A on at least three Ser residues in the RXXS motifs and that this phosphorylation is required, in part, for ERK-induced Xe-Cdc25A degradation.

Phosphorylation of Xe-Cdc25A by ERK

Our observations that even the RXXS:4A mutant is somewhat degraded after MEK-CA expression (Figure 2, A and C) and that Xe-Cdc25A WT is degraded more efficiently after MEK-CA expression than after p90rsk-CA expression (Figure 2C), suggest that some other kinase(s), in addition to p90rsk, is involved in the MEK-CA-induced phosphorylation and degradation of Xe-Cdc25A. If so, the other kinase could be ERK itself, because MEK-CA expression induced a stronger phosphorylation (as well as degradation) of Xe-Cdc25A than p90rsk-CA expression (Figure 2C) and this phosphorylation (as well as degradation) was completely

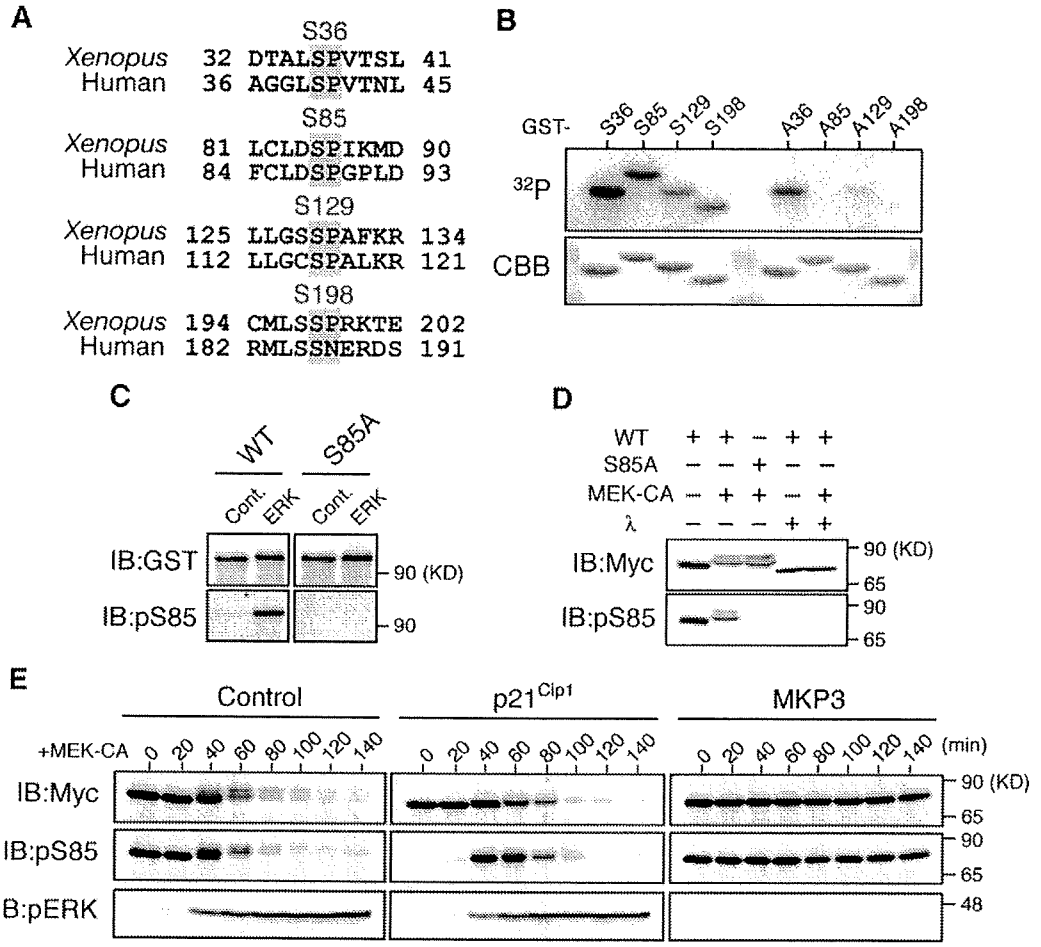

Figure 3. Phosphorylation of Xe-Cdc25A by ERK. (A) Conservation of consensus ERK phosphorylation motifs (Ser-Pro) in *Xenopus* and human Cdc25A proteins. (B) The indicated GST-fused Xe-Cdc25A peptides were incubated with [γ-^{32}P]ATP and ERK protein and analyzed as described in Figure 2B. (C) GST-tagged full-length Xe-Cdc25A proteins (WT or S85A) were synthesized in wheat germ extracts, purified by GST-pull-down, incubated with either buffer (Cont.) or ERK protein, and analyzed by immunoblotting with anti-GST and anti-phospho-S85 antibodies. (D) Activated eggs were injected with 2 ng of mRNA encoding Myc-Xe-Cdc25A (WT or S85A), reinjected or not 2.5 h later with 9 ng of MEK-CA mRNA, and cultured for 50 min. Egg extracts were treated or not with λ-phosphatase and analyzed for Myc-Xe-Cdc25A and phospho-S85 by immunoblotting. (E) Activated eggs were injected with either buffer (Control), 18 ng of p21^{Cip1} mRNA, or 9 ng of MKP3 mRNA, reinjected 40 min later with 2 ng of Myc-Xe-Cdc25A mRNA, further injected 2.5 h later with 9 ng of MEK-CA mRNA, collected at the indicated times, and analyzed by immunoblotting as described in D. Four, three, four, and five independent experiments were performed for B, C, D, and E, respectively, and, for each, a typical result is shown.

inhibited by ERK inactivation by MKP3 (Figure 1D). Interestingly, Xe-Cdc25A has four Ser residues (S36, S85, S129, and S198) that lie in the ERK consensus phosphorylation motif (Ser/Thr-Pro) and are mostly conserved in human Cdc25A (Figure 3A). Therefore, we first examined whether these four Ser residues could be phosphorylated by ERK in vitro, using [γ-^{32}P]ATP and GST-fused Xe-Cdc25A peptides, essentially as performed earlier for p90rsk (Figure 2B). As shown in Figure 3B, ERK was able to phosphorylate all of the four Ser residues, particularly S85, in vitro.

Because S85 and its equivalent site S88 are required for the Chk1-induced degradations of Xe-Cdc25A and human Cdc25A, respectively (Busino *et al.*, 2003; Kanemori *et al.*, 2005), we investigated S85 phosphorylation by ERK in more detail. When phosphorylated by ERK in vitro, GST-fused full-length Xe-Cdc25A WT, but not its S85A mutant, was efficiently recognized by anti-phospho-S85 antibody (Figure 3C), confirming that S85 of Xe-Cdc25A can be phosphorylated by ERK in vitro. We then analyzed S85 phosphorylation in vivo. When coexpressed with MEK-CA in activated eggs, Xe-Cdc25A WT, but not the S85A mutant, was recognized by the anti-phospho-S85 antibody in a manner sensitive to λ-phosphatase treatment (Figure 3D). Surprisingly, however, S85 phosphorylation was detected even in the absence of MEK-CA expression (Figure 3D; see also time 0 in Figure 3E, Cont.) and after MEK-CA expression in the presence of pre-expressed MKP3 (Figure 3E, MKP3). Interestingly, this unexpected phosphorylation was strongly inhibited by prior expression of the Cdk inhibitor p21^{Cip1} (see times 0 and 20 min in Figure 3E, p21^{Cip1}), indicating that it was mediated by Cdk, another proline-directed kinase. Importantly, however, despite the presence of p21^{Cip1}, S85 phosphorylation did occur concurrently with ERK activation (and during Xe-Cdc25A degradation) after MEK-CA expression (see times 40–80 min in Figure 3E, p21^{Cip1}); this result was even clearer when the stable D231A mutant,

instead of the WT, was used for the analysis (Supplemental Figure S1A). Thus, these results show that ERK can directly phosphorylate Xe-Cdc25A on S85 both in vitro and in vivo and also on S36, S129, and S198 at least in vitro.

Contribution of ERK-catalyzed Phosphorylation to Xe-Cdc25A Degradation

To examine the requirement of ERK-catalyzed phosphorylations for Xe-Cdc25A degradation, we constructed several Xe-Cdc25A mutants, i.e., four single-Ala mutants (S36A, S85A, S129A, and S198A) and one quadruple-Ala mutant (S36/85/129/198A, termed SP:4A), and expressed them in activated eggs. After MEK-CA expression, the S129A mutant was as unstable as the WT, but both the S36A and S198A mutants were slightly more stable than the WT, and both the S85A and SP:4A mutants were significantly more stable than the WT (Figure 4A). In addition, reversion of Ala-129 to Ser (in SP:4A) had no appreciable effect on the stability of the SP:4A mutant, but reversion of Ala-36, Ala-85, or Ala-198 to Ser, particularly that of Ala-85 to Ser, significantly destabilized the SP:4A mutant (Figure 4B). Thus, these results suggest that most of the ERK-catalyzed phosphorylations, particularly phosphorylation at S85, contribute to the MEK-CA–induced degradation of Xe-Cdc25A.

As for S85 phosphorylation, this phosphorylation was probably mediated in part by Cdk (Figure 3E, $p21^{Cip1}$; Supplemental Figure S1A). However, even without Cdk activity (or in the presence of $p21^{Cip1}$), ERK activation was able to efficiently induce the degradation of Xe-Cdc25A WT (Figure 3E, $p21^{Cip1}$) but not of the S85A mutant (Supplemental Figure S1B). Thus, although Cdk also phosphorylates S85, ERK-catalyzed S85 phosphorylation alone is sufficient for the S85 phosphorylation-dependent degradation of Xe-Cdc25A.

We also compared stabilities of the SP:4A mutant, the p90rsk phosphorylation site mutant (RXXS:4A), the RXXS:4A/SP:4A double mutant (8A), and the β-TrCP binding site mutant (D231A) after MEK-CA expression. The SP:4A mutant was somewhat less stable than the completely stable D231A mutant (Figure 4C). The RXXS:4A mutant was also somewhat less stable than the D231A mutant (Figure 4C), consistent with earlier results (Figure 2A). However, the double 8A mutant was very stable, comparable with the D231A mutant (Figure 4C). Thus, these results strongly suggest that ERK phosphorylation and p90rsk phosphorylation contribute, roughly equally and additively, to the MEK-CA–induced degradation of Xe-Cdc25A. Significantly, by similar analyses, we also obtained evidence that ERK and p90rsk phosphorylations can target human Cdc25A for $SCF^{\beta\text{-}TrCP}$-dependent degradation in activated *Xenopus* eggs (Supplemental Figure S2).

ERK Pathway-dependent Degradation of Xe-Cdc25A during Oocyte Maturation

Given our results, Cdc25A might be degraded in an $SCF^{\beta\text{-}TrCP}$-dependent manner under physiological conditions in which the endogenous ERK pathway is strongly activated. During oocyte maturation in many species, the endogenous ERK pathway becomes fully activated under the control of Mos (which activates MEK) and plays an important role for meiotic division of the oocyte (Sagata, 1997; Kishimoto, 2003). Interestingly, a recent study in mice showed that Cdc25A present in immature oocytes is degraded during oocyte maturation, although the degradation mechanism is not known (Solc *et al.*, 2008). We therefore asked whether Xe-Cdc25A could be degraded in an $SCF^{\beta\text{-}TrCP}$- and ERK pathway-dependent manner during *Xenopus* oocyte maturation. Somewhat surprisingly, unlike in mice (Solc *et al.*, 2008),

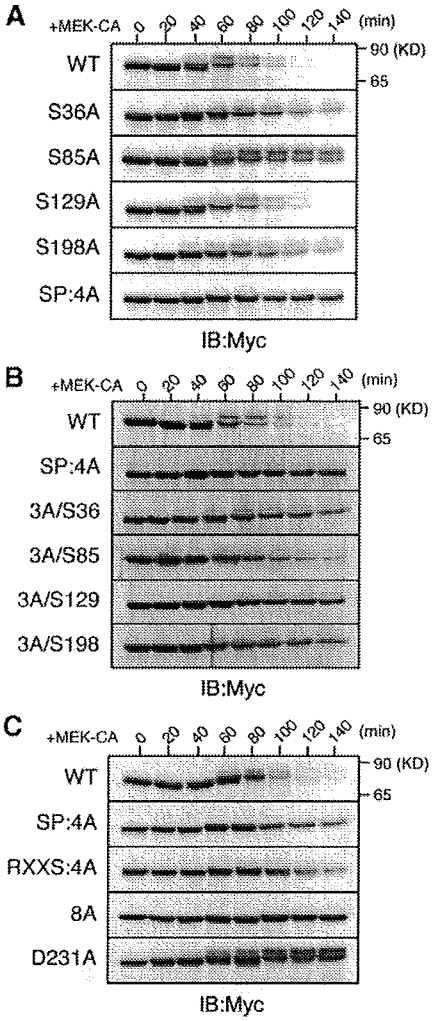

Figure 4. Requirement of ERK phosphorylation for Xe-Cdc25A degradation. (A–C) Activated eggs were injected with 2 ng of mRNA encoding the indicated Myc-Xe-Cdc25A constructs, reinjected 2.5 h later with 9 ng of MEK-CA mRNA, and analyzed for Myc-Xe-Cdc25A constructs by immunoblotting. In B, 3A/S36, etc., are reversion mutants of SP:4A (see text). Four independent experiments were performed for A–C, and, for each, a typical result is shown.

endogenous Xe-Cdc25A was not present in immature *Xenopus* oocytes, although it was present after fertilization, as reported previously (Kim *et al.*, 1999) (Figure 5A; also see Figure 1, A–C). Interestingly, however, ectopically expressed Xe-Cdc25A was readily detected in immature oocytes and was degraded during progesterone-induced oocyte maturation, coincidently with germinal vesicle breakdown (a hallmark for entry into meiosis I) (Figure 5B, Control) and ERK activation (Figure 5C, Control). Importantly, this degradation of Xe-Cdc25A was dependent on both $SCF^{\beta\text{-}TrCP}$ and ERK activity, because it was prevented either by overexpression of a dominant-negative mutant of β-TrCP (Figure 5B, β-TrCPΔF) or by treatment of the oocytes with the MEK-specific inhibitor U0126 (Figure 5C). Furthermore, and notably, both the RXXS:4A and SP:4A mutants were significantly more stable than Xe-Cdc25A WT, whereas both the double mutant (8A) and the β-TrCP-nonbinding

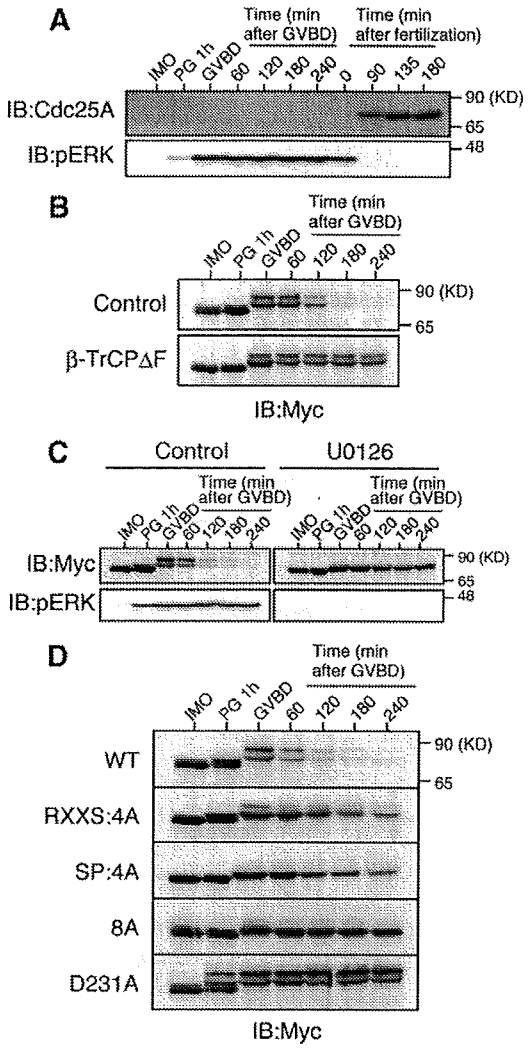

Figure 5. ERK pathway-dependent degradation of Xe-Cdc25A during oocyte maturation. (A) Immature oocytes (IMO) were treated with progesterone (PG) to induce maturation, whereas ovulated eggs were fertilized in vitro. Maturing oocytes and fertilized eggs were collected at the indicated times, and analyzed for endogenous Xe-Cdc25A and phospho-ERK by immunoblotting. GVBD denotes germinal vesicle breakdown. (B) Immature oocytes were coinjected with 2 ng of Myc-Xe-Cdc25A mRNA and 20 ng of either GST mRNA (Control) or β-TrCPΔF mRNA, cultured overnight, treated with progesterone, and analyzed for Myc-Xe-Cdc25A by immunoblotting. (C) Immature oocytes were injected with 2 ng of Myc-Xe-Cdc25A mRNA, cultured overnight, pretreated with dimethyl sulfoxide (Control) or 100 μM U0126 for 1 h, treated with progesterone, and analyzed for Myc-Xe-Cdc25A and phospho-ERK by immunoblotting. (D) Immature oocytes were injected with 2 ng of mRNA encoding the indicated Myc-Xe-Cdc25A constructs, cultured overnight, treated with progesterone, and analyzed for Myc-Xe-Cdc25A constructs by immunoblotting. In B–D, all the Myc-Xe-Cdc25A constructs were, in fact, phosphatase-dead C428S forms to avoid premature maturation of the oocytes. Four, three, four, and five independent experiments were performed for A, B, C, and D, respectively, and, for each, a typical result is shown.

mutant D231A were nearly completely stable, during oocyte maturation (Figure 5D). Additionally, the relative stabilities of these mutants during oocyte maturation were essentially the same as those observed in activated eggs expressing MEK-CA (compare Figures 4C and 5D). Thus, most probably, both ERK and p90rsk in the Mos–MEK–ERK–p90rsk pathway, as well as $SCF^{\beta\text{-}TrCP}$, are involved in the degradation of (ectopic) Xe-Cdc25A during oocyte maturation. These results suggest that, even under physiological conditions, a strongly activated ERK pathway can target coexisting Cdc25A for $SCF^{\beta\text{-}TrCP}$-dependent degradation.

Cell Cycle Arrest by ERK-induced Xe-Cdc25A Degradation

Cdc25A dephosphorylates Cdk1/Cdk2 on Thr-14/Tyr-15 residues and thereby promotes cell cycle progression in mammalian cells (Hoffmann *et al.*, 1994; Molinari *et al.*, 2000). Xe-Cdc25A begins to be synthesized after fertilization or egg activation (Figure 5A; Kim *et al.*, 1999) and is involved in the rapid embryonic cell cycles (Kim *et al.*, 1999). To determine whether ERK-induced Xe-Cdc25A degradation can elicit cell cycle arrest at interphase as does Chk1-induced Cdc25A degradation (Mailand *et al.*, 2000; Shimuta *et al.*, 2002; Busino *et al.*, 2003), we ectopically expressed MEK-CA in one-cell embryos, and then monitored the inhibitory T14/Y15 phosphorylation of Cdk1 as well as the external morphology of embryos (Shimuta *et al.*, 2002). In this experiment, however, we used embryos depleted of endogenous Erp1 (a maternal meiotic inhibitor) by antisense morpholino oligos (Figure 6A), because this maternal factor, if present and phosphorylated by p90rsk, induces metaphase arrest of the embryo owing to its cytostatic factor activity (Inoue *et al.*, 2007; Nishiyama *et al.*, 2007). Expression of MEK-CA in Erp1-depleted embryos induced both the degradation of endogenous Xe-Cdc25A and the T14/Y15 phosphorylation of Cdk1 (Figure 6B); remarkably, it also induced cleavage arrest of the embryos at the two/four-cell stages (Figure 6C). Thus, ERK activation can induce cell cycle arrest at interphase in early embryos.

To test whether the cell cycle arrest by ERK activation was a result of ERK-induced Xe-Cdc25A degradation, we coexpressed MEK-CA and either Xe-Cdc25A WT or its stable 8A mutant in Erp1-depleted embryos. Under the present experimental conditions (see Figure 6B legend), coexpression of Xe-Cdc25A WT did not appreciably affect Cdk1 T14/Y15 phosphorylation or cleavage arrest induced by MEK-CA expression. However, coexpression of the stable 8A mutant greatly reduced the levels of Cdk1 T14/Y15 phosphorylation (Figure 6B) and largely restored embryonic cell divisions (Figure 6C). Thus, clearly, the stable 8A mutant, but not the WT, can overcome ERK-induced cell cycle arrest, indicating that Xe-Cdc25A degradation is responsible for the ERK-induced cell cycle arrest. These results suggest that strong ERK activation can induce cell cycle arrest at interphase by targeting Cdc25A for degradation.

DISCUSSION

Chk1 phosphorylates and targets Cdc25A for $SCF^{\beta\text{-}TrCP}$-dependent degradation both in mammalian cells and *Xenopus* embryos (Busino *et al.*, 2003; Jin *et al.*, 2003; Kanemori *et al.*, 2005). In this study, we have found that the ERK pathway can also phosphorylate and target Xe-Cdc25A for $SCF^{\beta\text{-}TrCP}$-dependent degradation in *Xenopus* eggs. Interestingly, the mechanism of Xe-Cdc25A degradation induced by the ERK pathway is very similar to that induced by Chk1, as summarized in Figure 7.

Our results show that, when strongly activated in *Xenopus* eggs, the ERK–MAPK pathway, but not the JNK or p38 MAPK pathways, can induce prominent phosphorylation and degradation of Xe-Cdc25A (Figure 1, A and B). This